further suggests the possibility of developing a novel therapeutic measure to eliminate HCV by the exogenous expression of VAP-C in the hepatocytes of chronic hepatitis C patients.

ACKNOWLEDGMENTS

We thank H. Murase for her secretarial work. We also thank R. Bartenschlager and T. Wakita for providing cell lines and plasmids.

This work was supported in part by grants-in-aid from the Ministry of Health, Labor, and Welfare; the Ministry of Education, Culture, Sports, Science, and Technology; the Global Center of Excellence Program; and the Foundation for Biomedical Research and Innovation.

REFERENCES

1. **Abe, T., Y. Kaname, I. Hamamoto, Y. Tsuda, X. Wen, S. Taguwa, K. Moriishi, O. Takeuchi, T. Kawai, T. Kanto, N. Hayashi, S. Akira, and Y. Matsuura.** 2007. Hepatitis C Virus nonstructural protein 5A modulates Toll-like receptor-MyD88-dependent signaling pathway in the macrophage cell lines. J. Virol. **81:**8953–8966.
2. **Aizaki, H., K. J. Lee, V. M. Sung, H. Ishiko, and M. M. Lai.** 2004. Characterization of the hepatitis C virus RNA replication complex associated with lipid rafts. Virology **324:**450–461.
3. **Behrens, S. E., L. Tomei, and R. De Francesco.** 1996. Identification and properties of the RNA-dependent RNA polymerase of hepatitis C virus. EMBO J. **15:**12–22.
4. **Blight, K. J., A. A. Kolykhalov, and C. M. Rice.** 2000. Efficient initiation of HCV RNA replication in cell culture. Science **290:**1972–1974.
5. **Egger, D., B. Wolk, R. Gosert, L. Bianchi, H. E. Blum, D. Moradpour, and K. Bienz.** 2002. Expression of hepatitis C virus proteins induces distinct membrane alterations including a candidate viral replication complex. J. Virol. **76:**5974–5984.
6. **Evans, M. J., C. M. Rice, and S. P. Goff.** 2004. Phosphorylation of hepatitis C virus nonstructural protein 5A modulates its protein interactions and viral RNA replication. Proc. Natl. Acad. Sci. USA **101:**13038–13043.
7. **Gao, L., H. Aizaki, J.-W. He, and M. M. C. Lai.** 2004. Interactions between viral nonstructural proteins and host protein hVAP-33 mediate the formation of hepatitis C virus RNA replication complex on lipid raft. J. Virol. **78:**3480–3488.
8. **Grakoui, A., D. W. McCourt, C. Wychowski, S. M. Feinstone, and C. M. Rice.** 1993. Characterization of the hepatitis C virus-encoded serine proteinase: determination of proteinase-dependent polyprotein cleavage sites. J. Virol. **67:**2832–2843.
9. **Hamamoto, I., Y. Nishimura, T. Okamoto, H. Aizaki, M. Liu, Y. Mori, T. Abe, T. Suzuki, M. M. Lai, T. Miyamura, K. Moriishi, and Y. Matsuura.** 2005. Human VAP-B is involved in hepatitis C virus replication through interaction with NS5A and NS5B. J. Virol. **79:**13473–13482.
10. **Hanada, K., K. Kumagai, S. Yasuda, Y. Miura, M. Kawano, M. Fukasawa, and M. Nishijima.** 2003. Molecular machinery for non-vesicular trafficking of ceramide. Nature **426:**803–809.
11. **Ho, S. N., H. D. Hunt, R. M. Horton, J. K. Pullen, and L. R. Pease.** 1989. Site-directed mutagenesis by overlap extension using the polymerase chain reaction. Gene **77:**51–59.
12. **Hoofnagle, J. H.** 2002. Course and outcome of hepatitis C. Hepatology **36:**S21–S29.
13. **Huang, D. C., S. Cory, and A. Strasser.** 1997. Bcl-2, Bcl-XL and adenovirus protein E1B19kD are functionally equivalent in their ability to inhibit cell death. Oncogene **14:**405–414.
14. **Ikeda, M., K. Abe, M. Yamada, H. Dansako, K. Naka, and N. Kato.** 2006. Different anti-HCV profiles of statins and their potential for combination therapy with interferon. Hepatology **44:**117–125.
15. **Inoue, K., T. Umehara, U. T. Ruegg, F. Yasui, T. Watanabe, H. Yasuda, J. M. Dumont, P. Scalfaro, M. Yoshiba, and M. Kohara.** 2007. Evaluation of a cyclophilin inhibitor in hepatitis C virus-infected chimeric mice in vivo. Hepatology **45:**921–928.
16. **Kaiser, S. E., J. H. Brickner, A. R. Reilein, T. D. Fenn, P. Walter, and A. T. Brunger.** 2005. Structural basis of FFAT motif-mediated ER targeting. Structure **13:**1035–1045.
17. **Kanekura, K., I. Nishimoto, S. Aiso, and M. Matsuoka.** 2006. Characterization of amyotrophic lateral sclerosis-linked P56S mutation of vesicle-associated membrane protein-associated protein B (VAPB/ALS8). J. Biol. Chem. **281:**30223–30233.
18. **Kapadia, S. B., and F. V. Chisari.** 2005. Hepatitis C virus RNA replication is regulated by host geranylgeranylation and fatty acids. Proc. Natl. Acad. Sci. USA **102:**2561–2566.
19. **Kawano, M., K. Kumagai, M. Nishijima, and K. Hanada.** 2006. Efficient trafficking of ceramide from the endoplasmic reticulum to the Golgi apparatus requires a VAMP-associated protein-interacting FFAT motif of CERT. J. Biol. Chem. **281:**30279–30288.
20. **Loewen, C. J., A. Roy, and T. P. Levine.** 2003. A conserved ER targeting motif in three families of lipid binding proteins and in Opi1p binds VAP. EMBO J. **22:**2025–2035.
21. **Lohmann, V., F. Korner, J. Koch, U. Herian, L. Theilmann, and R. Bartenschlager.** 1999. Replication of subgenomic hepatitis C virus RNAs in a hepatoma cell line. Science **285:**110–113.
22. **Lotz, G. P., A. Brychzy, S. Heinz, and W. M. Obermann.** 2008. A novel HSP90 chaperone complex regulates intracellular vesicle transport. J. Cell Sci. **121:**717–723.
23. **McLauchlan, J., M. K. Lemberg, G. Hope, and B. Martoglio.** 2002. Intramembrane proteolysis promotes trafficking of hepatitis C virus core protein to lipid droplets. EMBO J. **21:**3980–3988.
24. **Miyanari, Y., M. Hijikata, M. Yamaji, M. Hosaka, H. Takahashi, and K. Shimotohno.** 2003. Hepatitis C virus non-structural proteins in the probable membranous compartment function in viral genome replication. J. Biol. Chem. **278:**50301–50308.
25. **Moriishi, K., and Y. Matsuura.** 2007. Host factors involved in the replication of hepatitis C virus. Rev. Med. Virol. **17:**343–354.
26. **Moriishi, K., and Y. Matsuura.** 2003. Mechanisms of hepatitis C virus infection. Antivir. Chem. Chemother. **14:**285–297.
27. **Moriishi, K., T. Okabayashi, K. Nakai, K. Moriya, K. Koike, S. Murata, T. Chiba, K. Tanaka, R. Suzuki, T. Suzuki, T. Miyamura, and Y. Matsuura.** 2003. Proteasome activator PA28gamma-dependent nuclear retention and degradation of hepatitis C virus core protein. J. Virol. **77:**10237–10249.
28. **Nakagawa, S., T. Umehara, C. Matsuda, S. Kuge, M. Sudoh, and M. Kohara.** 2007. Hsp90 inhibitors suppress HCV replication in replicon cells and humanized liver mice. Biochem. Biophys. Res. Commun. **353:**882–888.
29. **Nishimura, A. L., M. Mitne-Neto, H. C. Silva, A. Richieri-Costa, S. Middleton, D. Cascio, F. Kok, J. R. Oliveira, T. Gillingwater, J. Webb, P. Skehel, and M. Zatz.** 2004. A mutation in the vesicle-trafficking protein VAPB causes late-onset spinal muscular atrophy and amyotrophic lateral sclerosis. Am. J. Hum. Genet. **75:**822–831.
30. **Nishimura, Y., M. Hayashi, H. Inada, and T. Tanaka.** 1999. Molecular cloning and characterization of mammalian homologues of vesicle-associated membrane protein-associated (VAMP-associated) proteins. Biochem. Biophys. Res. Commun. **254:**21–26.
31. **Niwa, H., K. Yamamura, and J. Miyazaki.** 1991. Efficient selection for high-expression transfectants with a novel eukaryotic vector. Gene **108:**193–199.
32. **Okamoto, K., Y. Mori, Y. Komoda, T. Okamoto, M. Okochi, M. Takeda, T. Suzuki, K. Moriishi, and Y. Matsuura.** 2008. Intramembrane processing by signal peptide peptidase regulates the membrane localization of hepatitis C virus core protein and viral propagation. J. Virol. **82:**8349–8361.
33. **Okamoto, K., K. Moriishi, T. Miyamura, and Y. Matsuura.** 2004. Intramembrane proteolysis and endoplasmic reticulum retention of hepatitis C virus core protein. J. Virol. **78:**6370–6380.
34. **Okamoto, T., Y. Nishimura, T. Ichimura, K. Suzuki, T. Miyamura, T. Suzuki, K. Moriishi, and Y. Matsuura.** 2006. Hepatitis C virus RNA replication is regulated by FKBP8 and Hsp90. EMBO J. **25:**5015–5025.
35. **Okamoto, T., H. Omori, Y. Kaname, T. Abe, Y. Nishimura, T. Suzuki, T. Miyamura, T. Yoshimori, K. Moriishi, and Y. Matsuura.** 2008. A single-amino-acid mutation in hepatitis C virus NS5A disrupting FKBP8 interaction impairs viral replication. J. Virol. **82:**3480–3489.
36. **Pennetta, G., P. R. Hiesinger, R. Fabian-Fine, I. A. Meinertzhagen, and H. J. Bellen.** 2002. Drosophila VAP-33A directs bouton formation at neuromuscular junctions in a dosage-dependent manner. Neuron **35:**291–306.
37. **Prosser, D. C., D. Tran, P. Y. Gougeon, C. Verly, and J. K. Ngsee.** 2008. FFAT rescues VAPA-mediated inhibition of ER-to-Golgi transport and VAPB-mediated ER aggregation. J. Cell Sci. **121:**3052–3061.
38. **Skehel, P. A., R. Fabian-Fine, and E. R. Kandel.** 2000. Mouse VAP33 is associated with the endoplasmic reticulum and microtubules. Proc. Natl. Acad. Sci. USA **97:**1101–1106.
39. **Skehel, P. A., K. C. Martin, E. R. Kandel, and D. Bartsch.** 1995. A VAMP-binding protein from *Aplysia* required for neurotransmitter release. Science **269:**1580–1583.
40. **Taguwa, S., T. Okamoto, T. Abe, Y. Mori, T. Suzuki, K. Moriishi, and Y. Matsuura.** 2008. Human butyrate-induced transcript 1 interacts with hepatitis C virus NS5A and regulates viral replication. J. Virol. **82:**2631–2641.
41. **Tellinghuisen, T. L., J. Marcotrigiano, and C. M. Rice.** 2005. Structure of the zinc-binding domain of an essential component of the hepatitis C virus replicase. Nature **435:**374–379.
42. **Tomei, L., C. Failla, E. Santolini, R. De Francesco, and N. La Monica.** 1993. NS3 is a serine protease required for processing of hepatitis C virus polyprotein. J. Virol. **67:**4017–4026.
43. **Tsuda, H., S. M. Han, Y. Yang, C. Tong, Y. Q. Lin, K. Mohan, C. Haueter, A. Zoghbi, Y. Harati, J. Kwan, M. A. Miller, and H. J. Bellen.** 2008. The amyotrophic lateral sclerosis 8 protein VAPB is cleaved, secreted, and acts as a ligand for Eph receptors. Cell **133:**963–977.
44. **Tu, H., L. Gao, S. T. Shi, D. R. Taylor, T. Yang, A. K. Mircheff, Y. Wen, A. E. Gorbalenya, S. B. Hwang, and M. M. Lai.** 1999. Hepatitis C virus RNA polymerase and NS5A complex with a SNARE-like protein. Virology **263:**30–41.

Downloaded from jvi.asm.org at Osaka University on July 21, 2009

45. **Ujino, S., S. Yamaguchi, K. Shimotohno, and H. Takaku.** 2009. Heat-shock protein 90 is essential for stabilization of the hepatitis C virus non-structural protein NS3. J. Biol. Chem. **284:**6841–6846.
46. **Wang, C., M. Gale, Jr., B. C. Keller, H. Huang, M. S. Brown, J. L. Goldstein, and J. Ye.** 2005. Identification of FBL2 as a geranylgeranylated cellular protein required for hepatitis C virus RNA replication. Mol. Cell **18:**425–434.
47. **Wasley, A., and M. J. Alter.** 2000. Epidemiology of hepatitis C: geographic differences and temporal trends. Semin. Liver Dis. **20:**1–16.
48. **Watashi, K., N. Ishii, M. Hijikata, D. Inoue, T. Murata, Y. Miyanari, and K. Shimotohno.** 2005. Cyclophilin B is a functional regulator of hepatitis C virus RNA polymerase. Mol. Cell **19:**111–122.
49. **Weir, M. L., A. Klip, and W. S. Trimble.** 1998. Identification of a human homologue of the vesicle-associated membrane protein (VAMP)-associated protein of 33 kDa (VAP-33): a broadly expressed protein that binds to VAMP. Biochem. J. **333:**247–251.
50. **Weir, M. L., H. Xie, A. Klip, and W. S. Trimble.** 2001. VAP-A binds promiscuously to both v- and tSNAREs. Biochem. Biophys. Res. Commun. **286:**616–621.
51. **Zhong, J., P. Gastaminza, G. Cheng, S. Kapadia, T. Kato, D. R. Burton, S. F. Wieland, S. L. Uprichard, T. Wakita, and F. V. Chisari.** 2005. Robust hepatitis C virus infection in vitro. Proc. Natl. Acad. Sci. USA **102:**9294–9299.

Downloaded from jvi.asm.org at Osaka University on July 21, 2009

JOURNAL OF VIROLOGY, Aug. 2009, p. 7629–7640
0022-538X/09/$08.00+0 doi:10.1128/JVI.00679-09
Copyright © 2009, American Society for Microbiology. All Rights Reserved.
Vol. 83, No. 15

Baculovirus Induces Type I Interferon Production through Toll-Like Receptor-Dependent and -Independent Pathways in a Cell-Type-Specific Manner[▽]

Takayuki Abe,[1] Yuuki Kaname,[1] Xiaoyu Wen,[1] Hideki Tani,[1] Kohji Moriishi,[1] Satoshi Uematsu,[2] Osamu Takeuchi,[2] Ken J. Ishii,[2] Taro Kawai,[2] Shizuo Akira,[2] and Yoshiharu Matsuura[1]*

Department of Molecular Virology, Research Institute for Microbial Diseases,[1] and Laboratory of Host Defense, WPI Immunology Frontier Research Center,[2] Osaka University, Osaka, Japan

Received 2 April 2009/Accepted 19 May 2009

***Autographa californica* nuclear polyhedrosis virus (AcNPV) is a double-stranded-DNA virus that is pathogenic to insects. AcNPV was shown to induce an innate immune response in mammalian immune cells and to confer protection of mice from lethal viral infection. In this study, we have shown that production of type I interferon (IFN) by AcNPV in murine plasmacytoid dendritic cells (pDCs) and non-pDCs, such as peritoneal macrophages and splenic CD11c$^+$ DCs, was mediated by Toll-like receptor (TLR)-dependent and -independent pathways, respectively. IFN regulatory factor 7 (IRF7) was shown to play a crucial role in the production of type I IFN by AcNPV not only in immune cells in vitro but also in vivo. In mouse embryonic fibroblasts (MEFs), AcNPV produced IFN-β and IFN-inducible chemokines through TLR-independent and IRF3-dependent pathways, in contrast to the TLR-dependent and IRF3/IRF7-independent production of proinflammatory cytokines. Although production of IFN-β and IFN-inducible chemokines was severely impaired in IFN promoter-stimulator 1 (IPS-1)-deficient MEFs upon infection with vesicular stomatitis virus, AcNPV produced substantial amounts of the cytokines in IPS-1-deficient MEFs. These results suggest that a novel signaling pathway(s) other than TLR- and IPS-1-dependent pathways participates in the production of type I IFN in response to AcNPV infection.**

The baculovirus *Autographa californica* nuclear polyhedrosis virus (AcNPV) is an enveloped, double-stranded-DNA (dsDNA) virus that is pathogenic primarily to insects. AcNPV has long been used as an efficient gene expression vector in insect cells (31, 35). Recently, baculovirus was shown to be capable of infecting various mammalian cells without any replication and of expressing foreign genes under the control of a mammalian promoter (28). Therefore, baculovirus is now recognized as a useful viral vector not only for abundant gene expression in insect cells but also for gene delivery into mammalian cells.

In addition to allowing efficient gene delivery, AcNPV has been shown to stimulate interferon (IFN) production in mammalian cell lines and confer protection from lethal virus infection in mice (2, 12). Furthermore, AcNPV was shown to possess a strong adjuvant activity to promote humoral and cellular immune responses against coadministered antigens, maturation of dendritic cells (DCs), and production of proinflammatory cytokines, chemokines, and type I IFNs (14). However, the precise mechanisms by which AcNPV induces a strong innate immune response in mice remain unclear. We have demonstrated previously that AcNPV activates the production of proinflammatory cytokines in peritoneal macrophages (PECs), splenic CD11c$^+$ DCs, and the murine macrophage line RAW264.7 through a Toll-like receptor 9 (TLR9)/MyD88-dependent pathway (1). However, significant amounts of IFN-α were still detectable in the PECs and splenic CD11c$^+$ DCs derived from TLR9- or MyD88-deficient mice in response to AcNPV, suggesting that TLR9/MyD88-independent pathways are involved in the production of type I IFN by AcNPV in the PECs and splenic CD11c$^+$ DCs (1).

Induction of type I IFN by pathogens is crucial for innate immunity, and such induction is mediated by the activation of pattern recognition receptors, such as TLRs and cytosolic receptors, including retinoic acid-inducible protein I (RIG-I) and melanoma differentiation-associated gene 5 (MDA5) (24, 49, 50). Type I IFN induction is controlled primarily at the gene transcriptional level, wherein a family of transcription factors, IFN regulatory factors (IRFs), plays a pivotal role (16). IRF3 and IRF7 are now known to be essential for the RIG-I-, MDA5-, and TLR-mediated type I IFN production pathway. IRF3 is induced by a primary response to initiate IFN-β production, whereas IRF7 is induced by IFN-β and participates in the late phase of IFN-α induction (16). All TLRs, except for TLR3, activate the MyD88-dependent pathway, whereas TLR3 and TLR4 activate the TRIF-dependent pathway. There is accumulating evidence that IRFs are activated by the MyD88- and TRIF-dependent signaling pathways and contribute to the activation of the type I IFN gene (24). RIG-I and MDA5 contain a C-terminal DExD/H-box RNA helicase domain required for the interaction with dsRNA and two N-terminal caspase recruitment and activation domains (CARDs) responsible for the activation of downstream IRF3, IRF7, and NF-κB signaling pathways (49).

Plasmacytoid DCs (pDCs) have been identified as the major cells involved in the production of type I IFN in response to viral stimulation (3, 6). The type I IFN production in the pDCs was dependent on the TLR signaling pathway, whereas that in non-pDC immune cells, including macrophages, conventional

* Corresponding author. Mailing address: Department of Molecular Virology, Research Institute for Microbial Diseases, Osaka University, 3-1 Yamada-oka, Suita, Osaka 565-0871, Japan. Phone: 81-6-6879-8340. Fax: 81-6-6879-8269. E-mail: matsuura@biken.osaka-u.ac.jp.

▽ Published ahead of print on 27 May 2009.

Downloaded from jvi.asm.org at Osaka University on July 7, 2009

DCs, and mouse embryonic fibroblasts (MEFs), was dependent on the RIG-I/MDA5 signaling pathways (23). On the other hand, recent studies have also shown that non-pDC immune cells participate in the production of type I IFN in response to viral infection through TLR-dependent and TLR-independent pathways (9, 34). Viral genomic DNA of adenovirus (38, 53) and herpes simplex virus type 1 (HSV-1) (15) produces type I IFN through both TLR-dependent and -independent pathways. Modified vaccinia virus Ankara has also been shown to induce TLR-independent type I IFN production (46). Furthermore, nonprofessional immune cells, such as fibroblasts, were shown to produce type I IFN upon viral infection through a TLR-independent pathway (23). Infection with intracellular bacteria or introduction of synthetic dsDNA also induces production of type I IFN through a TLR- or an RNA helicase-independent pathway (19), suggesting the existence of a cytosolic DNA-sensing mechanism which stimulates the production of type I IFN (4, 5, 43). These results suggest that genomes of DNA viruses and intracellular bacteria produce type I IFN through a not-yet-identified cytosolic DNA-sensing machinery.

In this study, we have examined the mechanism of production of type I IFN in both pDCs and non-pDCs in response to AcNPV stimulation. The levels of involvement of the TLR or the RNA helicase pathway in the production of type I IFN in response to AcNPV stimulation differed among cell types, and the production was completely dependent on IRF7 in both pDCs and non-pDCs, such as PECs and splenic CD11c$^+$ DCs, whereas it was dependent on IRF3 in MEFs. These results suggest that AcNPV is capable of producing type I IFN through both TLR9-dependent and -independent pathways and might be an ideal tool for elucidating the mechanisms of the induction of type I IFN by DNA in mammalian cells.

MATERIALS AND METHODS

Mice and MEFs. C57BL/6 mice were purchased from CLEA Japan (Tokyo, Japan). MyD88-, TLR3-, TLR7-, TLR9-, IFN-αβ receptor (IFNR)-, RIG-I-, or IFN promoter-stimulator 1 (IPS-1)-deficient mice and MEFs from mice with a double knockout of MyD88 and TRIF, RIG-I, or IPS-1 were described previously (13, 23, 30, 48). IRF3- and IRF7-deficient mice (18) were purchased from Riken BioResource Center (Tsukuba, Japan), and the MEFs from the deficient mice were obtained from day 12.5 to 13.5 embryos. MEFs were maintained in Dulbecco's modified Eagle's medium (Sigma, St. Louis, MO) supplemented with 10% heat-inactivated fetal calf serum, 1.5 mM L-glutamine, 100 U/ml penicillin, and 100 μg/ml streptomycin at 37°C in a humidified atmosphere, with 5% CO_2.

Viruses and reagents. AcNPV was propagated in *Spodoptera frugiperda* (Sf-9) cells in Sf-900II insect medium (Invitrogen, Tokyo, Japan) supplemented with 10% heat-inactivated fetal calf serum. AcNPV and viral DNA were purified as previously described (1). Phosphorothioate-stabilized mouse CpG (mCpG) oligodeoxynucleotides (ODN1668) (TCC-ATG-ACG-TTC-CTG-ATG-CT) were purchased from Invitrogen. Endotoxin-free bacterial DNA from *Escherichia coli* K-12, poly(I:C), and imiquimod (R-837), an imidazoquinoline amine analogue to guanosine, were purchased from InvivoGen (San Diego, CA). Lipopolysaccharide (LPS) derived from *Salmonella enterica* serovar Minnesota (Re-595) and chloroquine were purchased from Sigma. Vesicular stomatitis virus (VSV) variants GLPLF and NCP12.1, derived from Indiana strains, were kindly provided by M. A. Whitt (22). The virus stocks and the other TLR ligands were free of endotoxin (<0.01 endotoxin units/ml), as determined using a Pyrodick endotoxin measurement kit (Seikagaku Co., Tokyo, Japan).

Production of truncated forms of gp64 protein. A recombinant baculovirus possessing a cDNA encoding a deletion mutant of gp64 lacking a transmembrane region (gp64ΔTM) was produced as described previously (1) by using a Bac-to-Bac baculovirus expression system according to the manufacturer's instructions (Invitrogen). At 3 days after infection with the recombinant virus, the recombinant gp64 protein was purified from the culture supernatants by use of a column of nickel-nitrilotriacetic acid beads (Qiagen, Valencia, CA). The protein concentrations were determined by using a Micro BCA protein assay kit (Pierce, Rockford, IL). The recombinant proteins were analyzed by sodium dodecyl sulfate-12.5% polyacrylamide gel electrophoresis under reducing conditions, stained with GelCord Blue stain reagent (Pierce), and detected by immunoblot analysis using antihexahistidine monoclonal antibody (Santa Cruz Biotechnology, Santa Cruz, CA) or anti-gp64 (AcV5), kindly provided by P. Faulkner.

Preparation of PECs and splenic DCs. To evaluate cytokine production in macrophages in vitro, mice were intraperitoneally injected with 2 ml of 4% thioglycolate (Sigma), and exudation cells were harvested at 3 days posttreatment by peritoneal lavage. Thioglycolate-elicited PECs were seeded into 96-well plates at a concentration of 2×10^5 cells/well and treated with various doses of stimuli. After 24 h of incubation, culture supernatants were harvested and analyzed for cytokine production. To prepare splenocytes containing DCs or pDCs, spleen tissue was cut into small fragments and incubated with RPMI 1640 medium containing 400 U/ml collagenase (Wako, Tokyo, Japan) and 15 μg/ml DNase (Sigma) at 37°C for 20 min. For the last 5 min, 5 mM EDTA was added, and single-cell suspensions were prepared after red blood cell lysis. Splenic CD11c$^+$ DCs and pDCs were purified by a magnetic cell sorter system with anti-CD11c and anti-murine plasmacytoid dendritic cell antigen 1 microbeads (Miltenyi Biotec GmbH, Bergisch Gladbach, Germany), respectively, following the manufacturer's instructions. Enriched cells containing >90% splenic CD11c$^+$ DCs and pDCs were seeded into 96-well plates at a concentration of 2×10^5 cells/well.

Production of cytokines in vitro and in vivo. Production of IFNs (IFN-α and -β) and proinflammatory cytokines (interleukin-6 [IL-6] and IL-12) in the culture supernatants was determined by use of enzyme-linked immunosorbent assay (ELISA) kits purchased from PBL Biomedical Laboratories (New Brunswick, NJ) and BD PharMingen (San Diego, CA), respectively. To determine the effects of endosomal maturation on cytokine production by infection with AcNPV or transfection of baculoviral DNA, PECs and splenic CD11c$^+$ DCs were seeded into 96-well plates at a concentration of 2×10^5 cells/well and inoculated with AcNPV or transfected with the viral DNA encapsulated in liposomes in the presence or absence of endosomal inhibitors, such as chloroquine. AcNPV (100 μg/mouse) was intraperitoneally inoculated into wild-type mice and mice with knockout of the MyD88, TLR9, IFNR, or IRF7 gene, and levels of production of IL-12, IL-6, and IFN-α in sera were determined at different time points.

Quantitative analyses of cytokine mRNA. MEFs derived from wild-type mice; mice with knockout of the IRF3, IRF7, RIG-I, or IPS-1 gene; and mice with double knockout of the MyD88 and TRIF genes were stimulated with AcNPV, VSV, LPS, gp64ΔTM, AcNPV DNA, or poly(I:C). At 4 to 8 h posttreatment, total RNA was prepared from the MEFs by using an RNeasy mini kit (Qiagen). First-strand cDNA was synthesized by using a ReverTra Ace kit (Toyobo, Osaka, Japan) and an oligo(dT)$_{20}$ primer. Each cDNA was estimated by use of Platinum SYBR green qPCR SuperMix UDG (Invitrogen) according to the manufacturer's protocol. Fluorescent signals were analyzed with an ABI Prism 7000 instrument (Applied Biosystems, Tokyo, Japan). The mouse IFN-α1, IFN-β, MCP-1 (monocyte chemoattractant protein 1), IP-10, RANTES, IL-6, and GAPDH (glyceraldehyde-3-phosphate dehydrogenase) genes were amplified using the primer pairs 5′-AGCCTTGACACTCCTGGTACAAATG-3′ and 5′-TGGGTC AGCTCACTCAGGACA-3′, 5′-ACACCAGCCTGGCTTCCATC-3′ and 5′-TT GGAGCTGGAGCTGCTTATAGTTG-3′, 5′-GCATCCACGTGTTGGCTC A-3′ and 5′-CTCCAGCCTACTCATTGGGATCA-3′, 5′-TGAATCCGGAATC TAAGACCATCAA-3′ and 5′-AGGACTAGCCATCCACTGGGTAAAG-3′, 5′-GCTCAAGCCATCCTTGTGCTAA-3′ and 5′-CATTGAGCTGATGGAG GTC-3′, 5′-TTGGTTAAATGACCTGCAACAGGA-3′ and 5′-CCACTTCACA AGTCGGAGGCTTA-3′, and 5′-ACCACAGTCCATGCCATCAC-3′ and 5′-T CCACCACCCTGTTGCTGTA-3′, respectively. The expression of the mRNAs of each of the cytokines was normalized to that of GAPDH mRNA.

In vitro cytopathic-effect assays. Induction of an antiviral state by AcNPV in vitro was determined by the cytopathic-effect assay, as described previously (12). Briefly, MEFs seeded in triplicate in 96-well tissue culture plates (2×10^3 cells/well) were incubated with serial dilutions of AcNPV, poly(I:C), or mCpG and washed with medium after 24 h of incubation. Then, VSV (GLPLF strain) was inoculated at a multiplicity of infection (MOI) of 0.1. Cell viability was determined by crystal violet staining at 24 h postinfection.

RESULTS

Involvement of TLR-dependent and -independent pathways in the production of type I IFN by AcNPV in immune cells and in mice. We have reported previously that AcNPV is capable

Downloaded from jvi.asm.org at Osaka University on July 7, 2009

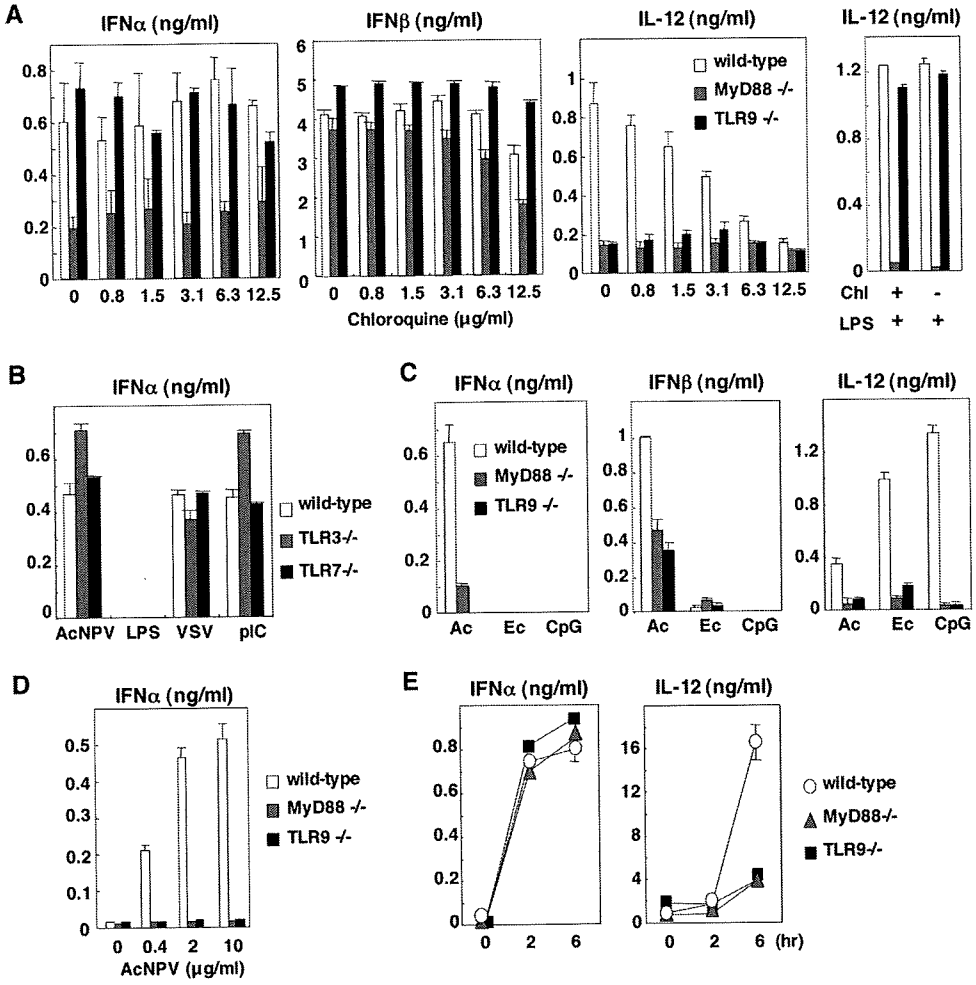

FIG. 1. Involvement of the TLR pathway in the production of type I IFN by AcNPV in immune cells and in mice. (A) PECs (2×10^5 cells/well) prepared from wild-type, MyD88-deficient, or TLR9-deficient mice were stimulated with AcNPV (10 μg/ml) at the indicated concentrations of chloroquine. These cells were also treated with LPS (10 μg/ml) in the presence (+) or absence (−) of chloroquine (Chl) (12.5 μg/ml) (right). After 24 h of incubation, the production of IFN-α, IFN-β, and IL-12 in culture supernatants was determined by ELISA. (B) PECs (2×10^5 cells/well) prepared from wild-type, TLR3-deficient, or TLR7-deficient mice were stimulated with AcNPV (10 μg/ml), LPS (10 μg/ml), VSV (NCP mutant, MOI of 0.1), or poly(I:C) (pIC) (50 μg/ml). After 24 h of incubation, production of IFN-α in culture supernatants was determined by ELISA. (C) PECs prepared as described for panel A were transfected with AcNPV DNA (Ac) (25 μg/ml), *E. coli* DNA (Ec) (25 μg/ml), or mCpG (CpG) (1 μg/ml). After 24 h of incubation, production of IFN-α, IFN-β, and IL-12 in the culture supernatants was determined by ELISA. (D) Splenic pDCs (2×10^5 cells/well) prepared from wild-type, MyD88-deficient, or TLR9-deficient mice were stimulated with AcNPV (10 μg/ml). After 24 h of incubation, production of IFN-α in the culture supernatants was determined by ELISA. (E) AcNPV (100 μg/mouse) was intraperitoneally inoculated into wild-type, MyD88-deficient, or TLR9-deficient mice, and levels of IFN-α and IL-12 production in sera were determined by ELISA at the indicated time points. Data are shown as the means ± standard deviations.

of producing type I IFN in PECs and splenic $CD11c^+$ DCs through a partially MyD88/TLR9-independent pathway (1). Although many studies of the production of type I IFN upon infection with DNA or RNA viruses have been conducted, the precise mechanisms of IFN production by AcNPV remain unclear. To clarify the mechanisms of induction of type I IFN by AcNPV in more detail, we examined the effect of inhibitors of endosomal maturation on the production of type I IFN by AcNPV in PECs derived from wild-type and MyD88- or TLR9-deficient mice. As shown in Fig. 1A, chloroquine clearly inhibited TLR9- or MyD88-dependent IL-12 production in PECs upon infection with AcNPV in a dose-dependent manner but not in cells from TLR9-deficient mice treated with LPS, probably due to the activation of TLR4 on the plasma membrane.

In contrast, AcNPV produces IFN-α and IFN-β through a TLR9-independent and partially MyD88-dependent pathway in PECs, whereas production of type I IFN by AcNPV in PECs was resistant to chloroquine treatment (Fig. 1A). These results indicate that AcNPV produces proinflammatory cytokines and type I IFN in PECs through a TLR-dependent and a TLR-independent pathway, respectively. Furthermore, AcNPV induces type I IFN in PECs through an endocytosis-independent pathway. AcNPV also produced type I IFN in $CD11c^+$ DCs through a TLR9-independent and partially MyD88-dependent pathway, as seen with the PECs, whereas type I IFN production in $CD11c^+$ DCs by AcNPV was sensitive to chloroquine treatment in a dose-dependent manner (data not shown). The partial impairment of IFN-α production in MyD88-deficient

Downloaded from jvi.asm.org at Osaka University on July 7, 2009

mice suggests that other TLRs may be involved in IFN production by AcNPV. However, PECs from mice deficient in TLR3 and TLR7, which recognize dsRNA and single-stranded RNA, respectively, exhibited no reduction of IFN-α production upon infection with AcNPV (Fig. 1B). These results suggest that a novel cytoplasmic DNA-sensing mechanism other than TLR3, TLR7, and TLR9 signaling pathways might be involved in the production of type I IFN in PECs upon infection with AcNPV.

Although AcNPV contains a high level of unmethylated CpG DNA comparable to that found in the genomes of *E. coli* and HSV (1), the involvement of a TLR9/MyD88 signal pathway in the production of type I IFN by the AcNPV genome remains unclear. *E. coli* DNA and phosphorothioate-stabilized mCpG oligonucleotides (ODN1668) were capable of producing a large amount of IL-12 in PECs through a TLR9/MyD88-dependent pathway, whereas production of type I IFN was not induced by the ligands (Fig. 1C). Production of IL-12 and IFN-α in PECs transfected with the purified baculoviral DNA was impaired by knockout of the TLR9 or the MyD88 gene, whereas substantial amounts of IFN-β were still produced in PECs derived from MyD88- or TLR9-deficient mice (Fig. 1C). These results suggest that a TLR9/MyD88-independent DNA recognition pathway participates in the production of type I IFN in PECs in response to the AcNPV genome.

pDCs are known as master producers of type I IFN upon virus infection, and IFN production is largely dependent on the TLR signaling pathway (11). IFN-α production in pDCs derived from TLR9- or MyD88-deficient mice was severely impaired in response to AcNPV stimulation (Fig. 1D), suggesting that AcNPV induces IFN-α production in pDCs through a TLR9/MyD88-dependent pathway. Next, to examine the mechanisms of induction of type I IFN by AcNPV in vivo, AcNPV was intraperitoneally inoculated into wild-type and MyD88- or TLR9-deficient mice, and levels of IFN-α and IL-12 production in sera were determined. TLR9- or MyD88-deficient mice exhibited a level of serum IFN-α similar to that of wild-type mice upon infection with AcNPV, whereas IL-12 production in the deficient mice was severely impaired (Fig. 1E). These results suggest that non-pDCs participate in the production of type I IFN through a TLR9/MyD88-independent pathway in response to AcNPV in vivo, in contrast to the TLR9/MyD88-dependent production of proinflammatory cytokines. Collectively, these results indicate that both TLR-dependent and -independent pathways are involved in the production of type I IFN in immune cells, including PECs, $CD11c^+$ DCs, and pDCs, in response to AcNPV.

IRF7 plays a crucial role in the production of type I IFN by AcNPV in immune cells and in mice. Both IRF3 and IRF7 are required for the production of type I IFN through a classical pathway activated by viral infection (18, 41). Therefore, we examined the involvement of IRF3 and IRF7 in the production of type I IFN in response to AcNPV by using PECs and splenic $CD11c^+$ DCs derived from IRF3- and IRF7-deficient mice (Fig. 2A). IFN-α production in the IRF7-deficient PECs and splenic $CD11c^+$ DCs in response to AcNPV or VSV was impaired, whereas such production was still active in the IRF3-deficient immune cells. IFN-β production in PECs was impaired in the IRF3- or IRF7-deficient mice in response to AcNPV, although significant amounts of IFN-β were produced in the IRF3- or IRF7-deficient PECs upon infection with VSV. In contrast to the PECs, IRF3-deficient splenic $CD11c^+$ DCs produced a level of IFN-β comparable to that in the wild-type cells in response to AcNPV. In response to VSV infection, production of IFN-β in the deficient immune cells was less impaired. Although enhancement of IL-12 production in the IRF3-deficient PECs and splenic $CD11c^+$ DCs in response to AcNPV or VSV was observed, similar levels of IL-12 production were observed in the IRF7-deficient immune cells and in wild-type cells in response to AcNPV or VSV.

There is circumstantial evidence that IRF7 plays a role in the MyD88-dependent production of IFN-α by activating the TLR in pDCs (17, 25). Therefore, we next examined the IFN-α production in pDCs obtained from IRF7-deficient mice. Consistent with the previous observations, IFN-α production in response to AcNPV was completely abolished in the IRF7-deficient pDCs (Fig. 2B). Furthermore, production of IFN-α, but not that of IL-12 and IL-6, in response to AcNPV in IRF7-deficient mice was severely impaired (Fig. 2C). These results suggest that IRF7 plays a crucial role in the production of type I IFN upon infection with AcNPV in the immune cells and in vivo.

Involvement of the IFNR signaling pathway in the production of type I IFN by AcNPV. The many subtypes of IFN-α and IFN-β are released from infected cells and bind to a single IFNR, and receptor-mediated signal transduction induces the expression of numerous IFN-stimulated genes whose products interfere with viral replication. To determine the involvement of the IFNR-mediated signal transduction in the induction of the innate immune response by AcNPV infection, production of IFN-α, IFN-β, and IL-12 in PECs and splenic $CD11c^+$ DCs derived from IFNR-deficient mice after stimulation with AcNPV or poly(I:C) was examined. Production of IFN-α and IFN-β was significantly impaired by AcNPV or poly(I:C) in the IFNR-deficient PECs and splenic $CD11c^+$ DCs (Fig. 3A and B), whereas IL-12 production in the deficient immune cells was comparable to that in the wild-type cells. In contrast to the in vitro data, production of IFN-α in the sera of IFNR-deficient mice was still detectable and exhibited a partial impairment at 6 h posttreatment (Fig. 3C). These results suggest that production of type I IFN in vitro in response to AcNPV is regulated mainly by an IFNR-mediated signal pathway, whereas an IFNR-independent pathway is additionally involved in the production of type I IFN in response to AcNPV in vivo.

Envelope glycoprotein gp64 does not participate in the immune activation by AcNPV. A previous study demonstrated that the recombinant envelope glycoprotein of AcNPV lacking a transmembrane domain (gp64ΔTM) did not produce proinflammatory cytokines or type I IFN in a murine macrophage cell line, RAW264.7 (1). However, the ability of gp64ΔTM to induce an innate immune response in primary mouse immune cells and nonimmune cells has not yet been examined. To determine the involvement of the envelope glycoprotein of AcNPV in immune activation, we prepared a C-terminally six-His-tagged gp64 lacking the transmembrane region (His-gp64ΔTM), as described previously (1), and examined its ability to activate primary mouse cells, such as PECs, splenic $CD11c^+$ DCs, and MEFs. His-gp64ΔTM was purified as a homogeneous band and was clearly detected by anti-His and anti-gp64 antibodies (Fig. 4A). Although infection with

Downloaded from jvi.asm.org at Osaka University on July 7, 2009

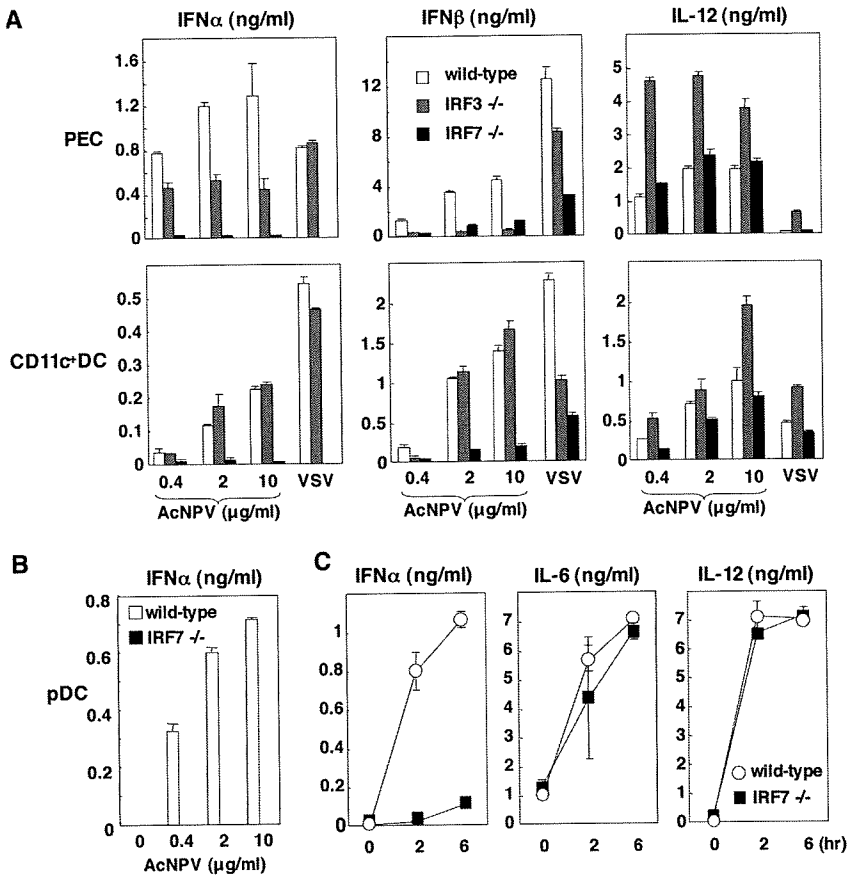

FIG. 2. IRF7 plays a crucial role in the production of type I IFN by AcNPV in immune cells and in mice. (A) PECs and splenic CD11c$^+$ DCs (2×10^5 cells/well) prepared from wild-type, IRF3-deficient, or IRF7-deficient mice were stimulated with the indicated amounts of AcNPV or VSV (NCP mutant, MOI of 0.1). After 24 h of incubation, the production of IFN-α, IFN-β, and IL-12 in culture supernatants was determined by ELISA. (B) Splenic pDCs (2×10^5 cells/well) prepared from wild-type or IRF7-deficient mice were stimulated with the indicated amounts of AcNPV. After 24 h of incubation, production of IFN-α in culture supernatants was determined by ELISA. (C) AcNPV (100 μg/mouse) was intraperitoneally inoculated into wild-type and IRF7-deficient mice, and levels of IL-12, IL-6, and IFN-α production in sera were determined by ELISA at the indicated times. Data are shown as the means ± standard deviations.

AcNPV produced large amounts of IL-12 and IFN-α in PECs and splenic CD11c$^+$ DCs, only a low level of IL-12 production was detected after infection with His-gp64ΔTM (Fig. 4B). Furthermore, infection with AcNPV resulted in rapid production of IFN-β, inflammatory cytokines, and chemokines, including IL-6, MCP-1, RANTES, and IP-10, in MEFs, in contrast to the low level of production of the cytokines by infection with His-gp64ΔTM (Fig. 4C). These results suggest that the envelope glycoprotein, gp64, does not play an important role in the immune activation by AcNPV.

AcNPV produces IFN-β and IFN-inducible chemokines through a TLR-independent and IRF3-dependent pathway in MEFs. We next examined the involvement of the TLR signaling pathway in immune activation by AcNPV in MEFs. MEFs were isolated from wild-type and MyD88/TRIF double knockout mice, and the production of cytokines after stimulation with AcNPV, VSV, LPS, or poly(I:C) was determined by ELISA and real-time PCR. In the MyD88/TRIF-deficient MEFs, the production of IL-6 was severely impaired in response to AcNPV and LPS, whereas no effect was observed after treatment with VSV or poly(I:C) (Fig. 5A, top). In contrast, the production of IFN-β in MEFs in response to AcNPV, VSV, or poly(I:C) was not affected by knockout of the MyD88/TRIF genes. LPS did not induce IFN-β production in either wild-type or MyD88/TRIF-deficient MEFs (Fig. 5A, bottom). Comparable levels of mRNA of IFN-β and IFN-inducible chemokines, including MCP-1, RANTES, and IP-10, were detected in wild-type and MyD88/TRIF knockout MEFs in response to AcNPV (Fig. 5B). These results suggest that a TLR-dependent pathway participates in the production of proinflammatory cytokines by AcNPV in MEFs, as seen with the immune cells, while AcNPV produces IFN-β and IFN-inducible chemokines in MEFs through a TLR-independent pathway.

Next, to determine the involvement of IRF3 and IRF7 in the immune activation in MEFs by AcNPV, wild-type and IRF3- or IRF7-deficient MEFs were treated with AcNPV, LPS, or VSV, and the production of cytokines was determined by ELISA and real-time PCR. Production of IL-6 in IRF3 or IRF7 knockout MEFs after treatment with AcNPV, VSV, or LPS was comparable to that in wild-type MEFs (Fig. 5C, top). In contrast, production of IFN-β was impaired in IRF3- and IRF7-deficient MEFs in response to AcNPV and VSV, respectively, while LPS induced no IFN production in either type of

Downloaded from jvi.asm.org at Osaka University on July 7, 2009

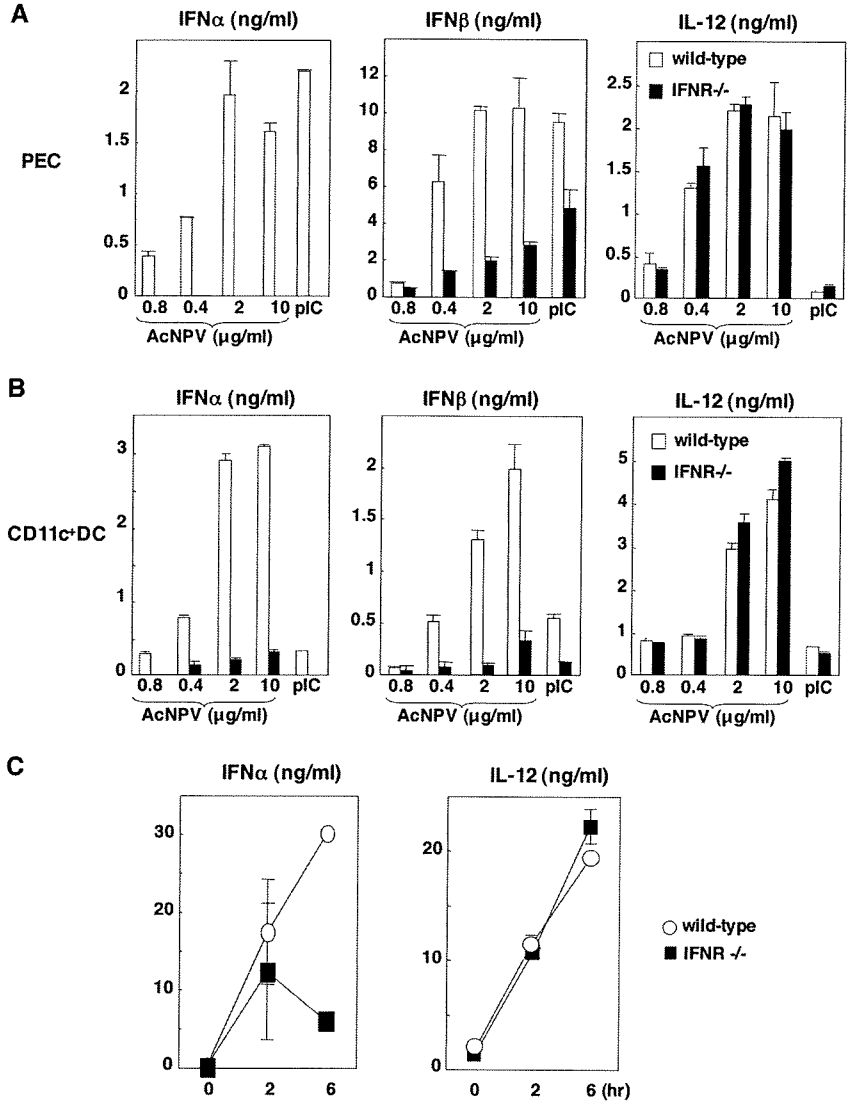

FIG. 3. Involvement of the IFNR signaling pathway in the production of type I IFN by AcNPV. (A and B) PECs (A) and splenic CD11c$^+$ DCs (B) (2×10^5 cells/well) prepared from wild-type and IFNR-deficient mice were stimulated with the indicated amounts of AcNPV or poly(I:C) (pIC) (50 μg/ml). After 24 h of incubation, the production of IFN-α, IFN-β, or IL-12 in culture supernatants was determined by ELISA. (C) AcNPV (100 μg/mouse) was intraperitoneally inoculated into wild-type and IFNR-deficient mice, and levels of IFN-α and IL-12 production in sera were determined by ELISA at the indicated time points. Data are shown as the means ± standard deviations.

MEF (Fig. 5C, bottom). Although robust transcription of IFN-β and IFN-inducible chemokines in response to AcNPV was detected in wild-type and IRF7-deficient MEFs, transcription of the genes in response to AcNPV was severely impaired in IRF3-deficient MEFs (Fig. 5D). These results indicate that AcNPV induces the production of IFN-β and IFN-inducible chemokines through a TLR-independent and IRF3-dependent pathway in MEFs, in contrast to the TLR-dependent and IRF3/IRF7-independent production of IL-6.

AcNPV induces antiviral status in MEFs through an IRF3-dependent pathway. To further examine the involvement of IRF3 in the induction of antiviral status in MEFs in response to AcNPV, wild-type and IRF3-deficient MEFs were transfected with the baculoviral DNA, and the mRNAs of the cytokines were measured. Transcription of IFN-β, IFN-α1, MCP-1, RANTES, and IP-10, but not that of IL-6, was impaired in IRF3-deficient MEFs upon transfection with baculoviral DNA (Fig. 6A).

To determine the involvement of endosomal maturation in the immune activation by AcNPV, the effect of chloroquine on the production of IFN-β and IL-6 in response to AcNPV or LPS was examined. Pretreatment with chloroquine reduced the secretion of IFN-β and IL-6 in MEFs in a dose-dependent manner in response to AcNPV infection but exhibited no effect on IL-6 production in MEFs by LPS treatment (Fig. 6B), suggesting that the impairment of IFN-β and IL-6 production was not due to the cytotoxicity of chloroquine. These results indicate that endosomal maturation is required for the induction of the innate immune response by AcNPV in MEFs.

Next, to determine the antiviral effects of the immune acti-

Downloaded from jvi.asm.org at Osaka University on July 7, 2009

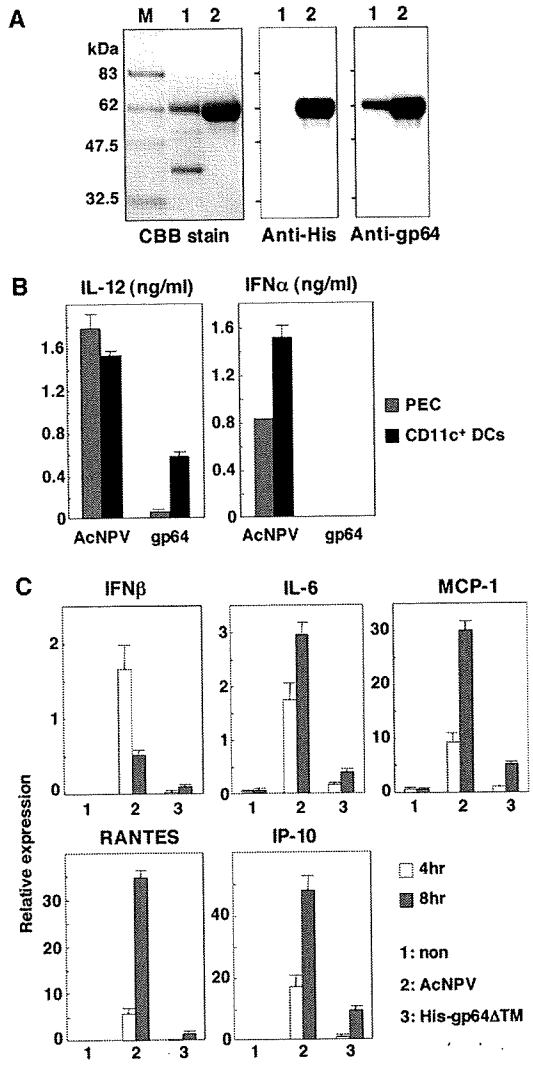

FIG. 4. Immune activation by AcNPV is not mediated by gp64. (A) His-gp64ΔTM expressed in Sf-9 cells was purified and subjected to sodium dodecyl sulfate-12.5% polyacrylamide gel electrophoresis under reducing conditions. Molecular size markers (lane M), purified AcNPV particles (lanes 1), and His-gp64ΔTM (lanes 2) were visualized by Coomassie blue (CBB) staining (left) and immunoblotting using antihexahistidine monoclonal antibody (middle) and anti-gp64 antibody (AcV5) (right). (B) PECs and splenic CD11c$^+$ DCs (2×10^5 cells/well) prepared from wild-type mice were stimulated with AcNPV (10 μg/ml) or His-gp64ΔTM (gp64) (20 μg/ml). After 24 h of incubation, production of IL-12 and IFN-α in culture supernatants was determined by ELISA. (C) MEFs (3×10^5 cells/well) prepared from wild-type mice were stimulated with AcNPV (10 μg/ml) or His-gp64ΔTM (20 μg/ml). At 4 h or 8 h poststimulation, total RNA was extracted and expression of mRNA of IFN-β, IL-6, MCP-1, RANTES, and IP-10 was determined by real-time PCR. Data are shown as the means ± standard deviations.

vation by AcNPV in MEFs, wild-type MEFs were pretreated with AcNPV or poly(I:C) and challenged with VSV (GLPLF mutant). Pretreatment with AcNPV (0.016 μg/ml to 2 μg/ml) or poly(I:C) (0.2 μg/ml to 25 μg/ml) conferred antiviral status against VSV infection in MEFs in a dose-dependent manner (Fig. 6C, left, and E). However, the induction of antiviral status by AcNPV or poly(I:C) treatment was completely abrogated in IRF3-deficient MEFs (Fig. 6C, right). On the other hand, pretreatment with IFN-α (10^1 to 10^4 U/ml) conferred antiviral status against VSV infection in both IRF knockout MEFs in a dose-dependent manner (Fig. 6D). These results clearly indicate that IRF3 plays a crucial role in the induction of antiviral status in MEFs by AcNPV.

Involvement of a TLR- and RIG-I/IPS-1-independent signaling pathway in immune activation by AcNPV. TLR3 has been shown to recognize viral dsRNA as well as a synthetic dsRNA analogue, poly(I:C), in the intracellular compartment. Recently, RIG-I and MDA5 have been identified as TLR-independent cytoplasmic RNA detectors and shown to induce type I IFN production through an adaptor molecule, IPS-1, that localizes in mitochondria (26, 36, 42, 47). To examine the involvement of TLR-independent cytoplasmic DNA-sensing machinery in the immune activation by AcNPV, as seen in the recognition of intracellular RNA, the production of type I IFN and IFN-inducible chemokines in PECs and splenic CD11c$^+$ DCs derived from RIG-I-, MDA5-, or IPS-1-deficient mice was examined. Type I IFN production in PECs and splenic CD11c$^+$ DCs in response to VSV and poly(I:C) was impaired by knockout of IPS-1, whereas AcNPV produced a significant amount of the IFNs in the IPS-1 knockout immune cells (Fig. 7A). Furthermore, IFN production in the immune cells in response to VSV was abrogated by knockout of the RIG-I gene but not by knockout of the MDA5 gene; however, AcNPV produced significant amounts of the IFNs in the RIG-I or MDA5 knockout immune cells (data not shown).

Next, to determine whether IPS-1 is involved in the production of type I IFN and IFN-inducible chemokines in MEFs in response to AcNPV, production of the cytokines in the IPS-1-deficient MEFs in response to VSV or AcNPV was examined (Fig. 7B). Production of IFN-β, IL-6, MCP-1, RANTES, and IP-10 was severely impaired in IPS-1-deficient MEFs upon VSV infection, whereas AcNPV produced substantial amounts of the cytokines in the IPS-1-deficient MEFs in spite of a slight reduction in IFN-β and IL-6 production (Fig. 7B). Similarly, production of the IFN-inducible chemokines in MEFs infected with VSV, but not with AcNPV, was also severely impaired by knockout of the RIG-I gene (data not shown). Collectively, these results suggest that a novel TLR- and RIG-I/IPS-1-independent signaling pathway(s) participated in the production of type I IFN and the IFN-inducible chemokines in both immunocompetent cells and MEFs in response to AcNPV infection.

DISCUSSION

Recent progress has been made in the identification of receptors, signal transduction molecules, and transcription factors that are required for the induction of type I IFN in cells upon infection with RNA and DNA viruses, as well as for the robust IFN production in pDCs, suggesting the presence of multiple signaling pathways for type I IFN induction (17, 23, 25). Production of type I IFN was shown to be induced through a number of different pathways in a cell-type-specific manner upon infection with HSV (40), although the precise mechanisms involved in sensing the foreign DNA of microorganisms remain largely unknown. In this study, we have examined the molecular mechanisms of type I IFN induction by AcNPV infection both in professional immune cells, including pDCs,

Downloaded from jvi.asm.org at Osaka University on July 7, 2009

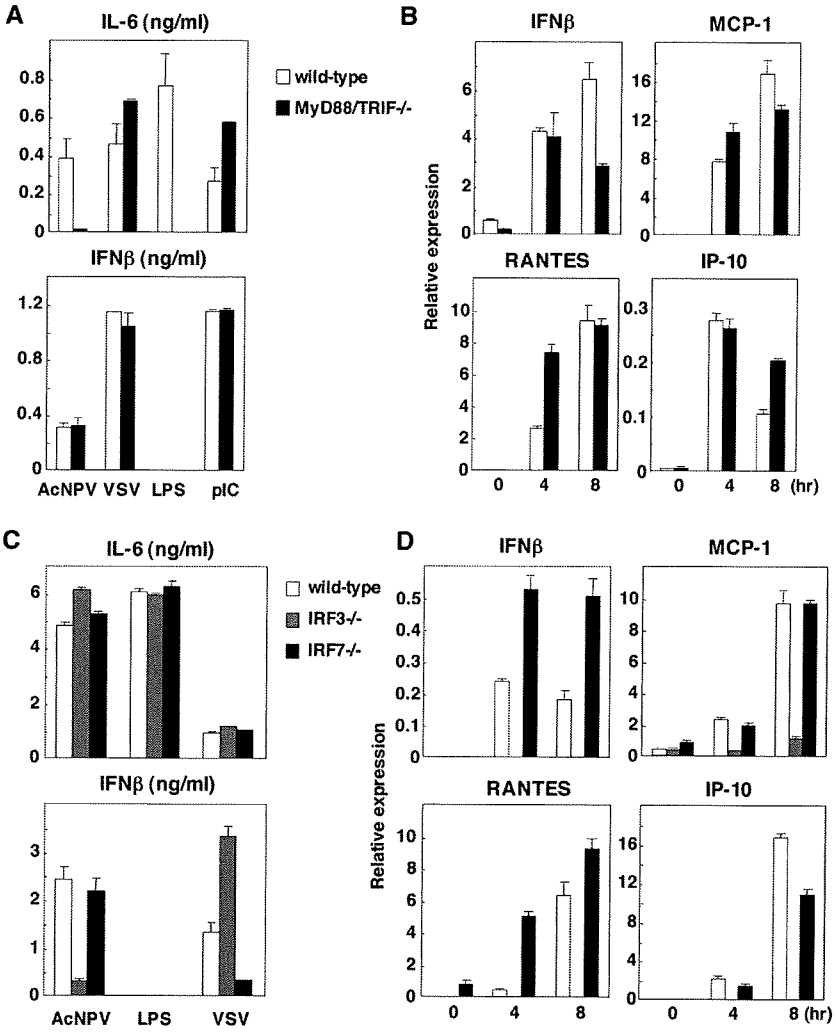

FIG. 5. AcNPV produces IFN-β and IFN-inducible chemokines through a TLR-independent and IRF3-dependent pathways in MEFs. (A) MEFs (2×10^4 cells/well) prepared from wild-type or MyD88/TRIF double knockout mice were stimulated with AcNPV (10 μg/ml), VSV (NCP mutant, MOI of 0.1), LPS (10 μg/ml), or poly(I:C) (pIC) (50 μg/ml). After 24 h of incubation, production of IL-6 and IFN-β in culture supernatants was determined by ELISA. (B) MEFs (3×10^5 cells/well) prepared from wild-type or MyD88/TRIF double knockout mice were stimulated with AcNPV (10 μg/ml). Total RNA was extracted at the indicated time points, and the expression of mRNA of IFN-β, MCP-1, RANTES, and IP-10 was determined by real-time PCR. (C) MEFs (2×10^4 cells/well) prepared from wild-type, IRF3-deficient, or IRF7-deficient mice were stimulated with AcNPV (10 μg/ml), LPS (10 μg/ml), or VSV (NCP mutant, MOI of 0.1). After 24 h of incubation, the production of IL-6 and IFN-β in culture supernatants was determined by ELISA. (D) MEFs (3×10^5 cells/well) prepared from wild-type, IRF3-deficient, or IRF7-deficient mice were stimulated with AcNPV (10 μg/ml). Total RNA was extracted at the indicated time points, and the expression of mRNA of IFN-β, MCP-1, RANTES, and IP-10 was determined by real-time PCR. Data are shown as the means ± standard deviations.

PECs, and splenic $CD11c^+$ DCs, and in nonimmune cells and raised the possibility of the involvement of a novel TLR- and IPS-1-independent pathway in the production of type I IFN in vitro as well as in vivo in response to AcNPV infection.

The frequency of bioactive CpG motifs capable of inducing immune activation through a TLR9-dependent pathway in the AcNPV genome was similar to that in *E. coli* and HSV and was significantly higher than that in entomopoxvirus (1, 51). Furthermore, it was shown that HSV and murine cytomegalovirus produce inflammatory cytokines and type I IFN through both TLR9-dependent and -independent pathways (7, 15, 29, 32, 44). Recently, it was also reported that adenovirus DNA produced IL-6 and IFN-α through an entirely TLR/MyD88-independent pathway in non-pDCs (53), although the presence of the CpG motifs in the adenoviral genome has not yet been determined. The current model of TLR9 activation by viral DNA is as follows. The virus particles are internalized into cells and degraded within the endocytic vesicles, and the digested viral genome subsequently actives TLR9 localized in the endosomal compartments. Treatment with inhibitors for endosomal maturation or acidification efficiently inhibits TLR7 and TLR9 activation by viral RNA and DNA, respectively (8, 32, 33). Interestingly, the production of type I IFN in PECs upon infection with AcNPV was resistant to pretreatment with endocytosis inhibitors, suggesting that the cytoplasmic recognition of AcNPV by TLR-independent immune sensors may be required for type I IFN production in PECs. The purified AcNPV DNA encapsulated in liposomes induced the produc-

Downloaded from jvi.asm.org at Osaka University on July 7, 2009

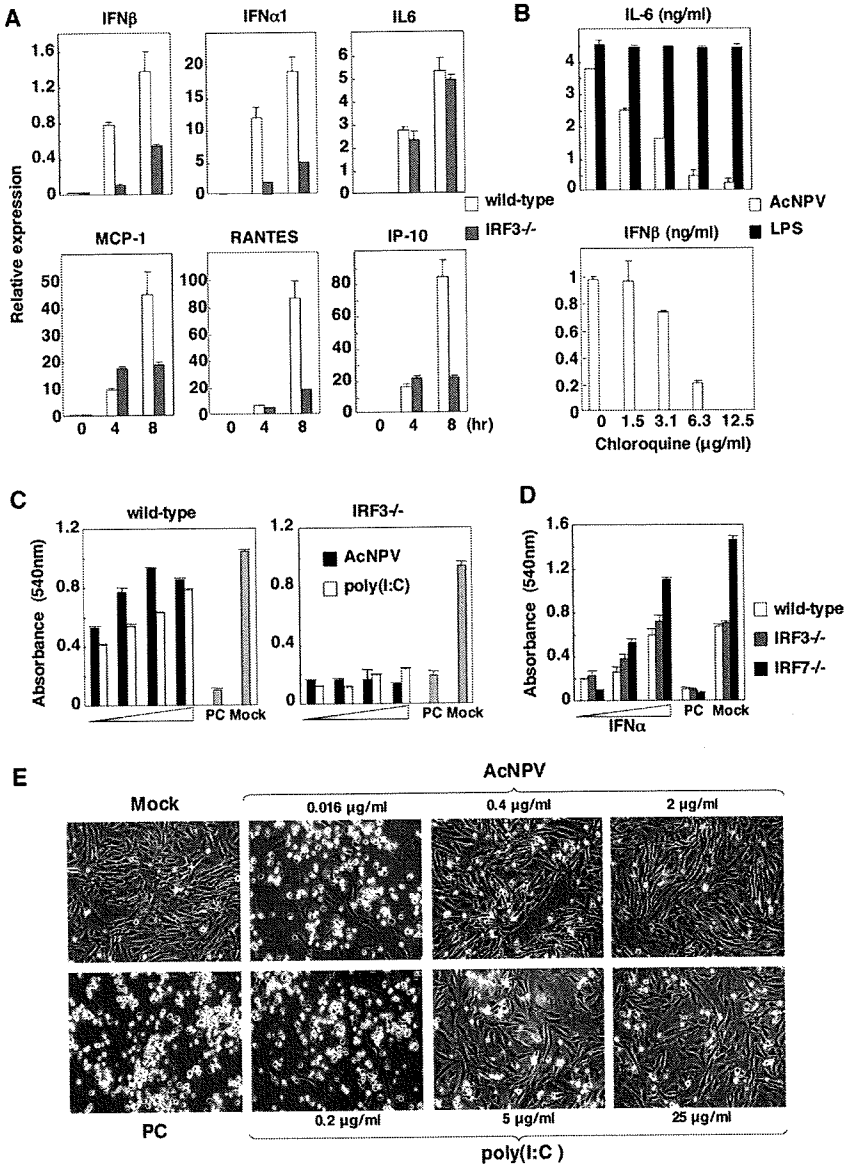

FIG. 6. AcNPV induces antiviral status in MEFs through an IRF3-dependent pathway. (A) MEFs (3×10^5 cells/well) prepared from wild-type and IRF3-deficient mice were transfected with AcNPV DNA (25 μg/ml). Total RNA was extracted at the indicated time points, and the expression of mRNA of IFN-β, IFN-α1, MCP-1, RANTES, IL-6, and IP-10 was determined by real-time PCR. (B) MEFs (2×10^4 cells/well) prepared from wild-type mice were stimulated with AcNPV (10 μg/ml) or LPS (10 μg/ml) in the presence of the indicated concentrations of chloroquine. After 24 h of incubation, production of IL-6 and IFN-β in culture supernatants was determined by ELISA. (C) MEFs (2×10^4 cells/well) prepared from wild-type and IRF3-deficient mice were incubated with AcNPV (0.016 μg/ml to 2 μg/ml) or poly(I:C) (0.2 μg/ml to 25 μg/ml). After 24 h of incubation, cells were washed extensively with warm medium and infected with VSV (GLPLF mutant, MOI of 0.1). Cell viability was determined at 24 h postinfection by crystal violet staining and quantitated by spectroscopy. (D) MEFs (2×10^4 cells/well) prepared from wild-type, IRF3-deficient, or IRF7-deficient mice were incubated with serial dilutions of murine IFN-α (10^1 to 10^4 U/ml). After 24 h of incubation, cells were washed extensively with warm medium and infected with VSV (GLPLF strain, MOI of 0.1). Cell viability was determined at 24 h postinfection by crystal violet staining and quantitated by spectroscopy. Values are plotted as means from the triplicate wells. Data are shown as means ± standard deviations. (E) Microscopic observation of MEFs from wild-type mice, showing the antiviral status against VSV infection by the treatment with AcNPV or poly(I:C) in a dose-dependent manner. PC, infected cells; Mock, mock-infected cells. Samples are shown at a magnification of ×40.

tion of type I IFN through both TLR9/MyD88-dependent and -independent pathways in PECs. These results indicate that the genomic DNA of AcNPV is recognized by at least two different pathways, TLR9-dependent endosomal recognition and TLR9-independent cytoplasmic recognition, and that type I IFN production by AcNPV is totally dependent on the latter process. However, the precise mechanisms of the immune activation of immunocompetent cells by AcNPV DNA through a TLR-independent pathway remain unknown. Therefore, further studies are needed to determine the molecular mechanisms underlying the type I IFN production through a TLR-independent cytoplasmic sensor for baculovirus DNA.

Downloaded from jvi.asm.org at Osaka University on July 7, 2009

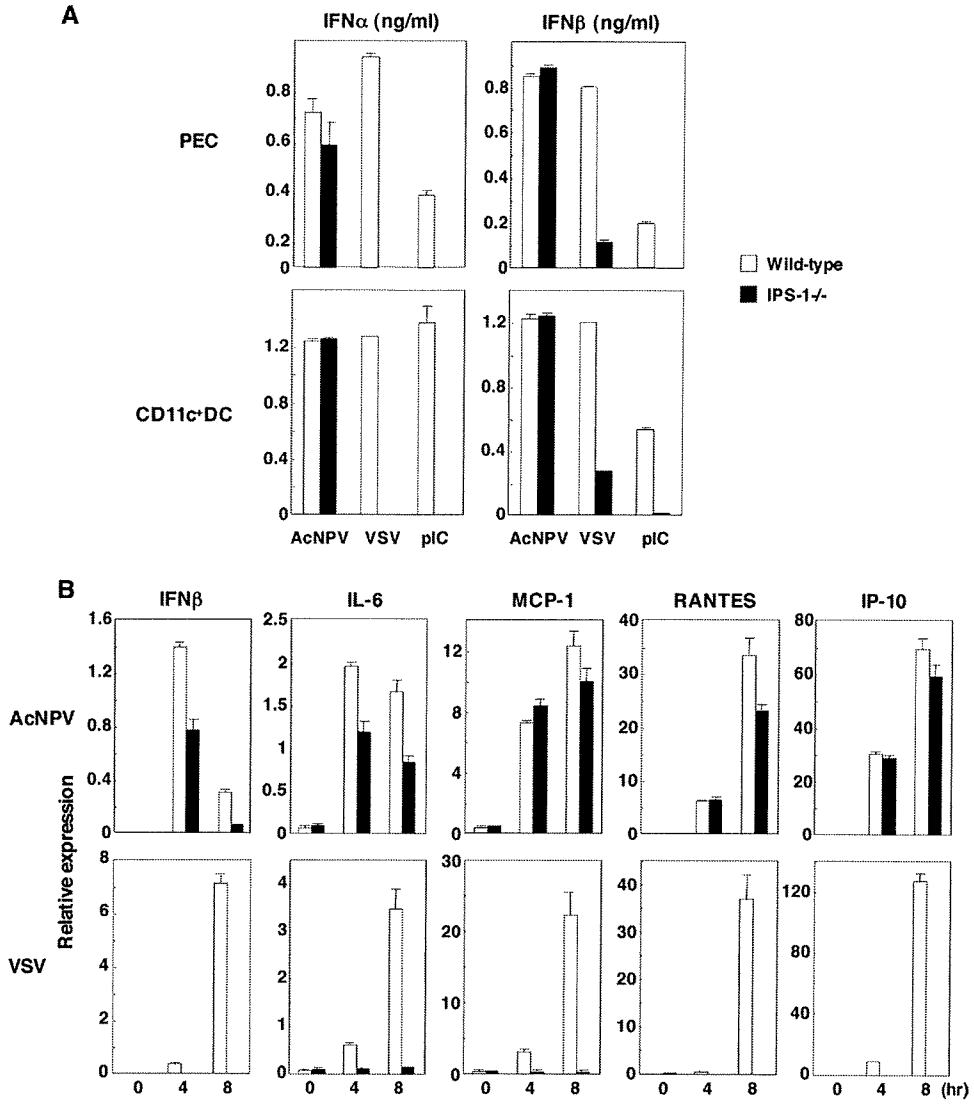

FIG. 7. Role of IPS-1 in immune activation by AcNPV. (A) PECs and splenic CD11c$^+$ DCs (2×10^5 cells/well) prepared from wild-type and IPS-1-deficient mice were stimulated with AcNPV (10 μg/ml), VSV (NCP mutant, MOI of 0.1), or poly(I:C) (pIC) (50 μg/ml). After 24 h of incubation, production of IFN-α and IFN-β in culture supernatants was determined by ELISA. (B) MEFs (3×10^5 cells/well) prepared from wild-type and IPS-1-deficient mice were stimulated with AcNPV (10 μg/ml) or VSV (NCP mutant, MOI of 0.1). Total RNA was extracted at the indicated time points, and the expression of mRNA of IFN-β, MCP-1, RANTES, IL-6, and IP-10 was determined by real-time PCR. Data are shown as the means ± standard deviations.

A novel TLR-independent cytosolic surveillance system for transfected dsDNA that elicits type I IFN induction through a TANK binding kinase 1 (TBK1)/IκB kinase-related kinase (IKKi)/IRF3 pathway has been shown to exist (19, 43). Our preliminary data also indicate that type I IFN production was severely reduced in TBK1-deficient MEFs in response to AcNPV and insufficient to protect cells from VSV infection (data not shown), suggesting the involvement of TBK1 in AcNPV-induced immune activation. Recently, a cytoplasmic recognition receptor, DAI (DNA-dependent activator of IRFs), was shown to be activated by dsDNA from a variety of sources and to produce type I IFN through an IRF3 and probably IRF7 pathway (45). However, there are conflicting reports suggesting a lack of impairment of type I IFN production in DAI knockout mice and DAI knockdown murine macrophages or MEFs in response to dsDNA of synthetic B-form DNA and from bacteria (4, 20). In this study, we have shown that splenic CD11c$^+$ DCs derived from IRF3-deficient mice produced a level of type I IFN compatible with that in wild-type mice in response to AcNPV, in contrast to the lack of IFN-β production in the PECs derived from the IRF3-deficient mice. More recently, two groups reported the identification of a membrane protein, termed mitochondrial mediator of IRF3 activation (MITA) or stimulator of IFN genes (STING), that activates IRF3 to induce a type I IFN response to viral infection (21, 52). Although both groups described slightly different characterizations of MITA, or STING, in terms of localization and signal transduction, both groups exhibited the opinion that MITA or STING plays a critical role in type I IFN production by B-form DNA. Although DAI-mediated type I IFN production was more

Downloaded from jvi.asm.org at Osaka University on July 7, 2009

dependent on IRF3 than on IRF7, the cytoplasmic DNA sensors, including DAI and MITA or STING, may participate in the induction of type I IFN upon infection with AcNPV.

In the cytoplasm, RIG-I and MDA5 are critically involved in the recognition of dsRNA, and the adaptor molecule IPS-1 interacts with RIG-I and MDA5 to facilitate TBK1- and IKKi-mediated IRF3 and IRF7 activation, which leads to termination of the replication of RNA viruses through the helicase function. In addition, RIG-I has been shown to discriminate viral RNAs from the vast number and variety of cellular RNAs by recognizing a terminal 5′ triphosphate, but not 5′ OH or a 5′ methylguanosine cap (37, 39). In this study, both RIG-I- and IPS-1-deficient MEFs but not immunocompetent cells partially impaired the production of IFN-β and IL-6, but not that of MCP-1, RANTES, and IP-10, in response to AcNPV, suggesting the possible generation of dsRNA in MEFs upon infection with AcNPV in spite of the lack of replication. Although there is no evidence for the functional expression of the viral proteins, transcription of immediate-early genes of baculovirus was detected in HeLa and BHK cells upon infection with AcNPV by DNA microarray analysis (10) and in HEK293 cells and rat primary Schwann cells upon infection with *Bombyx mori* NPV by reverse transcription-PCR (27). These reports are consistent with our observations that the RIG-I/IPS-1 pathway partially participates in type I IFN induction by AcNPV infection in MEFs.

We have shown previously that an intranasal inoculation of AcNPV induces protective immunity from a lethal challenge of influenza A virus in mice (2) and that AcNPV produces type I IFN in immune cells of mice via a TLR9/MyD88-independent pathway (1). Our present studies further confirmed that AcNPV induces a strong antiviral immunity through a TLR-independent pathway. Although further studies are needed to clarify the precise mechanisms underlying the antiviral responses, a TLR-independent and probably TBK1-IRF3/IRF7-dependent signaling pathway may contribute to the induction of protective immunity against viral challenge induced by AcNPV infection in vivo.

ACKNOWLEDGMENTS

We thank H. Murase for her secretarial work.

This work was supported in part by grants-in-aid from the Research and Development Program for New Bio-industry Initiatives of Bio-oriented Technology Research Advancement Institution (BRAIN) and the Ministry of Education, Culture, Sports, Science, and Technology, Japan.

We have no conflicting financial interests.

REFERENCES

1. **Abe, T., H. Hemmi, H. Miyamoto, K. Moriishi, S. Tamura, H. Takaku, S. Akira, and Y. Matsuura.** 2005. Involvement of the Toll-like receptor 9 signaling pathway in the induction of innate immunity by baculovirus. J. Virol. **79**:2847–2858.
2. **Abe, T., H. Takahashi, H. Hamazaki, N. Miyano-Kurosaki, Y. Matsuura, and H. Takaku.** 2003. Baculovirus induces an innate immune response and confers protection from lethal influenza virus infection in mice. J. Immunol. **171**:1133–1139.
3. **Bjorck, P.** 2001. Isolation and characterization of plasmacytoid dendritic cells from Flt3 ligand and granulocyte-macrophage colony-stimulating factor-treated mice. Blood **98**:3520–3526.
4. **Charrel-Dennis, M., E. Latz, K. A. Halmen, P. Trieu-Cuot, K. A. Fitzgerald, D. L. Kasper, and D. T. Golenbock.** 2008. TLR-independent type I interferon induction in response to an extracellular bacterial pathogen via intracellular recognition of its DNA. Cell Host Microbe **4**:543–554.
5. **Chessler, A. D., L. R. Ferreira, T. H. Chang, K. A. Fitzgerald, and B. A. Burleigh.** 2008. A novel IFN regulatory factor 3-dependent pathway activated by trypanosomes triggers IFN-beta in macrophages and fibroblasts. J. Immunol. **181**:7917–7924.
6. **Coccia, E. M., M. Severa, E. Giacomini, D. Monneron, M. E. Remoli, I. Julkunen, M. Cella, R. Lande, and G. Uze.** 2004. Viral infection and Toll-like receptor agonists induce a differential expression of type I and lambda interferons in human plasmacytoid and monocyte-derived dendritic cells. Eur. J. Immunol. **34**:796–805.
7. **Delale, T., A. Paquin, C. Asselin-Paturel, M. Dalod, G. Brizard, E. E. Bates, P. Kastner, S. Chan, S. Akira, A. Vicari, C. A. Biron, G. Trinchieri, and F. Briere.** 2005. MyD88-dependent and -independent murine cytomegalovirus sensing for IFN-alpha release and initiation of immune responses in vivo. J. Immunol. **175**:6723–6732.
8. **Diebold, S. S., T. Kaisho, H. Hemmi, S. Akira, and C. Reis e Sousa.** 2004. Innate antiviral responses by means of TLR7-mediated recognition of single-stranded RNA. Science **303**:1529–1531.
9. **Diebold, S. S., M. Montoya, H. Unger, L. Alexopoulou, P. Roy, L. E. Haswell, A. Al-Shamkhani, R. Flavell, P. Borrow, and C. Reis e Sousa.** 2003. Viral infection switches non-plasmacytoid dendritic cells into high interferon producers. Nature **424**:324–328.
10. **Fujita, R., T. Matsuyama, J. Yamagishi, K. Sahara, S. Asano, and H. Bando.** 2006. Expression of *Autographa californica* multiple nucleopolyhedrovirus genes in mammalian cells and upregulation of the host beta-actin gene. J. Virol. **80**:2390–2395.
11. **Gilliet, M., W. Cao, and Y. J. Liu.** 2008. Plasmacytoid dendritic cells: sensing nucleic acids in viral infection and autoimmune diseases. Nat. Rev. Immunol. **8**:594–606.
12. **Gronowski, A. M., D. M. Hilbert, K. C. Sheehan, G. Garotta, and R. D. Schreiber.** 1999. Baculovirus stimulates antiviral effects in mammalian cells. J. Virol. **73**:9944–9951.
13. **Hemmi, H., O. Takeuchi, T. Kawai, T. Kaisho, S. Sato, H. Sanjo, M. Matsumoto, K. Hoshino, H. Wagner, K. Takeda, and S. Akira.** 2000. A Toll-like receptor recognizes bacterial DNA. Nature **408**:740–745.
14. **Hervas-Stubbs, S., P. Rueda, L. Lopez, and C. Leclerc.** 2007. Insect baculoviruses strongly potentiate adaptive immune responses by inducing type I IFN. J. Immunol. **178**:2361–2369.
15. **Hochrein, H., B. Schlatter, M. O'Keeffe, C. Wagner, F. Schmitz, M. Schiemann, S. Bauer, M. Suter, and H. Wagner.** 2004. Herpes simplex virus type-1 induces IFN-alpha production via Toll-like receptor 9-dependent and -independent pathways. Proc. Natl. Acad. Sci. USA **101**:11416–11421.
16. **Honda, K., and T. Taniguchi.** 2006. IRFs: master regulators of signalling by Toll-like receptors and cytosolic pattern-recognition receptors. Nat. Rev. Immunol. **6**:644–658.
17. **Honda, K., H. Yanai, T. Mizutani, H. Negishi, N. Shimada, N. Suzuki, Y. Ohba, A. Takaoka, W. C. Yeh, and T. Taniguchi.** 2004. Role of a transductional-transcriptional processor complex involving MyD88 and IRF-7 in Toll-like receptor signaling. Proc. Natl. Acad. Sci. USA **101**:15416–15421.
18. **Honda, K., H. Yanai, H. Negishi, M. Asagiri, M. Sato, T. Mizutani, N. Shimada, Y. Ohba, A. Takaoka, N. Yoshida, and T. Taniguchi.** 2005. IRF-7 is the master regulator of type-I interferon-dependent immune responses. Nature **434**:772–777.
19. **Ishii, K. J., C. Coban, H. Kato, K. Takahashi, Y. Torii, F. Takeshita, H. Ludwig, G. Sutter, K. Suzuki, H. Hemmi, S. Sato, M. Yamamoto, S. Uematsu, T. Kawai, O. Takeuchi, and S. Akira.** 2006. A Toll-like receptor-independent antiviral response induced by double-stranded B-form DNA. Nat. Immunol. **7**:40–48.
20. **Ishii, K. J., T. Kawagoe, S. Koyama, K. Matsui, H. Kumar, T. Kawai, S. Uematsu, O. Takeuchi, F. Takeshita, C. Coban, and S. Akira.** 2008. TANK-binding kinase-1 delineates innate and adaptive immune responses to DNA vaccines. Nature **451**:725–729.
21. **Ishikawa, H., and G. N. Barber.** 2008. STING is an endoplasmic reticulum adaptor that facilitates innate immune signalling. Nature **455**:674–678.
22. **Jayakar, H. R., and M. A. Whitt.** 2002. Identification of two additional translation products from the matrix (M) gene that contribute to vesicular stomatitis virus cytopathology. J. Virol. **76**:8011–8018.
23. **Kato, H., S. Sato, M. Yoneyama, M. Yamamoto, S. Uematsu, K. Matsui, T. Tsujimura, K. Takeda, T. Fujita, O. Takeuchi, and S. Akira.** 2005. Cell type-specific involvement of RIG-I in antiviral response. Immunity **23**:19–28.
24. **Kawai, T., and S. Akira.** 2006. Innate immune recognition of viral infection. Nat. Immunol. **7**:131–137.
25. **Kawai, T., S. Sato, K. J. Ishii, C. Coban, H. Hemmi, M. Yamamoto, K. Terai, M. Matsuda, J. Inoue, S. Uematsu, O. Takeuchi, and S. Akira.** 2004. Interferon-alpha induction through Toll-like receptors involves a direct interaction of IRF7 with MyD88 and TRAF6. Nat. Immunol. **5**:1061–1068.
26. **Kawai, T., K. Takahashi, S. Sato, C. Coban, H. Kumar, H. Kato, K. J. Ishii, O. Takeuchi, and S. Akira.** 2005. IPS-1, an adaptor triggering RIG-I- and Mda5-mediated type I interferon induction. Nat. Immunol. **6**:981–988.
27. **Kenoutis, C., R. C. Efrose, L. Swevers, A. A. Lavdas, M. Gaitanou, R. Matsas, and K. Iatrou.** 2006. Baculovirus-mediated gene delivery into mammalian cells does not alter their transcriptional and differentiating potential but is accompanied by early viral gene expression. J. Virol. **80**:4135–4146.
28. **Kost, T. A., J. P. Condreay, and D. L. Jarvis.** 2005. Baculovirus as versatile

Downloaded from jvi.asm.org at Osaka University on July 7, 2009

vectors for protein expression in insect and mammalian cells. Nat. Biotechnol. **23**:567–575.
29. **Krug, A., G. D. Luker, W. Barchet, D. A. Leib, S. Akira, and M. Colonna.** 2004. Herpes simplex virus type 1 activates murine natural interferon-producing cells through toll-like receptor 9. Blood **103**:1433–1437.
30. **Kumar, H., T. Kawai, H. Kato, S. Sato, K. Takahashi, C. Coban, M. Yamamoto, S. Uematsu, K. J. Ishii, O. Takeuchi, and S. Akira.** 2006. Essential role of IPS-1 in innate immune responses against RNA viruses. J. Exp. Med. **203**:1795–1803.
31. **Luckow, V. A., and M. D. Summers.** 1988. Signals important for high-level expression of foreign genes in Autographa californica nuclear polyhedrosis virus expression vectors. Virology **167**:56–71.
32. **Lund, J., A. Sato, S. Akira, R. Medzhitov, and A. Iwasaki.** 2003. Toll-like receptor 9-mediated recognition of herpes simplex virus-2 by plasmacytoid dendritic cells. J. Exp. Med. **198**:513–520.
33. **Lund, J. M., L. Alexopoulou, A. Sato, M. Karow, N. C. Adams, N. W. Gale, A. Iwasaki, and R. A. Flavell.** 2004. Recognition of single-stranded RNA viruses by Toll-like receptor 7. Proc. Natl. Acad. Sci. USA **101**:5598–5603.
34. **Malmgaard, L., J. Melchjorsen, A. G. Bowie, S. C. Mogensen, and S. R. Paludan.** 2004. Viral activation of macrophages through TLR-dependent and -independent pathways. J. Immunol. **173**:6890–6898.
35. **Matsuura, Y., R. D. Possee, H. A. Overton, and D. H. Bishop.** 1987. Baculovirus expression vectors: the requirements for high level expression of proteins, including glycoproteins. J. Gen. Virol. **68**:1233–1250.
36. **Meylan, E., J. Curran, K. Hofmann, D. Moradpour, M. Binder, R. Bartenschlager, and J. Tschopp.** 2005. Cardif is an adaptor protein in the RIG-I antiviral pathway and is targeted by hepatitis C virus. Nature **437**:1167–1172.
37. **Nallagatla, S. R., J. Hwang, R. Toroney, X. Zheng, C. E. Cameron, and P. C. Bevilacqua.** 2007. 5′-triphosphate-dependent activation of PKR by RNAs with short stem-loops. Science **318**:1455–1458.
38. **Nociari, M., O. Ocheretina, J. W. Schoggins, and E. Falck-Pedersen.** 2007. Sensing infection by adenovirus: Toll-like receptor-independent viral DNA recognition signals activation of the interferon regulatory factor 3 master regulator. J. Virol. **81**:4145–4157.
39. **Pichlmair, A., O. Schulz, C. P. Tan, T. I. Naslund, P. Liljestrom, F. Weber, and C. Reis e Sousa.** 2006. RIG-I-mediated antiviral responses to single-stranded RNA bearing 5′-phosphates. Science **314**:997–1001.
40. **Rasmussen, S. B., L. N. Sorensen, L. Malmgaard, N. Ank, J. D. Baines, Z. J. Chen, and S. R. Paludan.** 2007. Type I interferon production during herpes simplex virus infection is controlled by cell-type-specific viral recognition through Toll-like receptor 9, the mitochondrial antiviral signaling protein pathway, and novel recognition systems. J. Virol. **81**:13315–13324.
41. **Sato, M., H. Suemori, N. Hata, M. Asagiri, K. Ogasawara, K. Nakao, T. Nakaya, M. Katsuki, S. Noguchi, N. Tanaka, and T. Taniguchi.** 2000. Distinct and essential roles of transcription factors IRF-3 and IRF-7 in response to viruses for IFN-alpha/beta gene induction. Immunity **13**:539–548.
42. **Seth, R. B., L. Sun, C. K. Ea, and Z. J. Chen.** 2005. Identification and characterization of MAVS, a mitochondrial antiviral signaling protein that activates NF-kappaB and IRF 3. Cell **122**:669–682.
43. **Stetson, D. B., and R. Medzhitov.** 2006. Recognition of cytosolic DNA activates an IRF3-dependent innate immune response. Immunity **24**:93–103.
44. **Tabeta, K., P. Georgel, E. Janssen, X. Du, K. Hoebe, K. Crozat, S. Mudd, L. Shamel, S. Sovath, J. Goode, L. Alexopoulou, R. A. Flavell, and B. Beutler.** 2004. Toll-like receptors 9 and 3 as essential components of innate immune defense against mouse cytomegalovirus infection. Proc. Natl. Acad. Sci. USA **101**:3516–3521.
45. **Takaoka, A., Z. Wang, M. K. Choi, H. Yanai, H. Negishi, T. Ban, Y. Lu, M. Miyagishi, T. Kodama, K. Honda, Y. Ohba, and T. Taniguchi.** 2007. DAI (DLM-1/ZBP1) is a cytosolic DNA sensor and an activator of innate immune response. Nature **448**:501–505.
46. **Waibler, Z., M. Anzaghe, H. Ludwig, S. Akira, S. Weiss, G. Sutter, and U. Kalinke.** 2007. Modified vaccinia virus Ankara induces Toll-like receptor-independent type I interferon responses. J. Virol. **81**:12102–12110.
47. **Xu, L. G., Y. Y. Wang, K. J. Han, L. Y. Li, Z. Zhai, and H. B. Shu.** 2005. VISA is an adapter protein required for virus-triggered IFN-beta signaling. Mol. Cell **19**:727–740.
48. **Yamamoto, M., S. Sato, H. Hemmi, K. Hoshino, T. Kaisho, H. Sanjo, O. Takeuchi, M. Sugiyama, M. Okabe, K. Takeda, and S. Akira.** 2003. Role of adaptor TRIF in the MyD88-independent toll-like receptor signaling pathway. Science **301**:640–643.
49. **Yoneyama, M., M. Kikuchi, K. Matsumoto, T. Imaizumi, M. Miyagishi, K. Taira, E. Foy, Y. M. Loo, M. Gale, Jr., S. Akira, S. Yonehara, A. Kato, and T. Fujita.** 2005. Shared and unique functions of the DExD/H-box helicases RIG-I, MDA5, and LGP2 in antiviral innate immunity. J. Immunol. **175**:2851–2858.
50. **Yoneyama, M., M. Kikuchi, T. Natsukawa, N. Shinobu, T. Imaizumi, M. Miyagishi, K. Taira, S. Akira, and T. Fujita.** 2004. The RNA helicase RIG-I has an essential function in double-stranded RNA-induced innate antiviral responses. Nat. Immunol. **5**:730–737.
51. **Zheng, M., D. M. Klinman, M. Gierynska, and B. T. Rouse.** 2002. DNA containing CpG motifs induces angiogenesis. Proc. Natl. Acad. Sci. USA **99**:8944–8949.
52. **Zhong, B., Y. Yang, S. Li, Y. Y. Wang, Y. Li, F. Diao, C. Lei, X. He, L. Zhang, P. Tien, and H. B. Shu.** 2008. The adaptor protein MITA links virus-sensing receptors to IRF3 transcription factor activation. Immunity **29**:538–550.
53. **Zhu, J., X. Huang, and Y. Yang.** 2007. Innate immune response to adenoviral vectors is mediated by both Toll-like receptor-dependent and -independent pathways. J. Virol. **81**:3170–3180.

Downloaded from jvi.asm.org at Osaka University on July 7, 2009

Hepatitis B Virus X Protein Shifts Human Hepatic Transforming Growth Factor (TGF)-β Signaling from Tumor Suppression to Oncogenesis in Early Chronic Hepatitis B

Miki Murata,[1] Koichi Matsuzaki,[1] Katsunori Yoshida,[1] Go Sekimoto,[1] Yoshiya Tahashi,[1] Shigeo Mori,[1] Yoshiko Uemura,[2] Noriko Sakaida,[2] Junichi Fujisawa,[3] Toshihito Seki,[1] Kazuki Kobayashi,[4] Koutaro Yokote,[4] Kazuhiko Koike,[5] and Kazuichi Okazaki[1]

Hepatitis B virus X (HBx) protein is suspected to participate in oncogenesis during chronic hepatitis B progression. Transforming growth factor β (TGF-β) signaling involves both tumor suppression and oncogenesis. TGF-β activates TGF-β type I receptor (TβRI) and c-Jun N-terminal kinase (JNK), which differentially phosphorylate the mediator Smad3 to become C-terminally phosphorylated Smad3 (pSmad3C) and linker-phosphorylated Smad3 (pSmad3L). Reversible shifting of Smad3-mediated signaling between tumor suppression and oncogenesis in HBx-expressing hepatocytes indicated that TβRI-dependent pSmad3C transmitted a tumor-suppressive TGF-β signal, while JNK-dependent pSmad3L promoted cell growth. We used immunostaining, immunoblotting, and *in vitro* kinase assay to compare pSmad3L- and pSmad3C-mediated signaling in biopsy specimens representing chronic hepatitis, cirrhosis, or hepatocellular carcinoma (HCC) from 90 patients chronically infected with hepatitis B virus (HBV) with signaling in liver specimens from HBx transgenic mice. In proportion to plasma HBV DNA levels, early chronic hepatitis B specimens showed prominence of pSmad3L in hepatocytic nuclei. HBx-activated JNK/pSmad3L/c-Myc oncogenic pathway was enhanced, while the TβRI/pSmad3C/p21^{WAF1} tumor-suppressive pathway was impaired as human and mouse HBx-associated hepatocarcinogenesis progressed. Of 28 patients with chronic hepatitis B who showed strong oncogenic pSmad3L signaling, six developed HCC within 12 years; only one of 32 patients showing little pSmad3L developed HCC. In contrast, seven of 30 patients with little Smad3C phosphorylation developed HCC, while no patient who retained hepatocytic tumor-suppressive pSmad3C developed HCC within 12 years. *Conclusion:* HBx shifts hepatocytic TGF-β signaling from the tumor-suppressive pSmad3C pathway to the oncogenic pSmad3L pathway in early carcinogenic process. Hepatocytic pSmad3L and pSmad3C assessment in HBV-infected liver specimens should prove clinically useful for predicting risk of HCC. (HEPATOLOGY 2009;49:1203-1217.)

Hepatocellular carcinoma (HCC) is the fifth most common cancer worldwide and one of the most deadly, causing approximately 600,000 deaths yearly.[1] The overall incidence of HCC continues to rise, especially in western Europe and the United States.[2] During the past 20 years, striking advances have enhanced our understanding of HCC. More than 85% of HCC cases are related to known hepatitis B virus (HBV) and hepatitis C virus (HCV).

Abbreviations: Ab, antibody; HBV, hepatitis B virus; HBx, hepatitis B virus X; HCC, hepatocellular carcinoma; HCV, hepatitis C virus; HSC, hepatic stellate cells; IgG, immunoglobulin G; JNK, c-Jun N-terminal kinase; PPM1A, protein phosphatase magnesium 1A; pSmad3C, C-terminally phosphorylated Smad3; pSmad3L, linker-phosphorylated Smad3; SCP1-3, small C-terminal domain phosphatase 1-3; TGF-β, transforming growth factor β; TβRI, TGF-β type I receptor; TβRII, TGF-β type II receptor.

From the Departments of [1]Gastroenterology and Hepatology, [2]Surgical Pathology, and [3]Microbiology, Kansai Medical University, Osaka, Japan; the [4]Department of Clinical Cell Biology, Chiba University Graduate School of Medicine, Chiba, Japan; and the [5]Department of Infectious Diseases, Internal Medicine, Graduate School of Medicine, University of Tokyo, Tokyo, Japan.

Received March 19, 2008; accepted November 25, 2008.

Supported by the Ministry of Education, Science, and Culture of Japan (K. M.).

A strong correlation between chronic HBV infection and HCC occurrence has long been apparent according to epidemiologic evidence and the finding of integrated HBV DNA sequences in virtually all HBV-related HCC.[3] Hepatitis B virus X (HBx) oncoprotein has been implicated in HBV-mediated hepatocarcinogenesis,[4,5] and persistent high-level expression of HBx protein in transgenic mouse liver results in hyperplasia leading to HCC, with no preceding inflammation.[6] Although HBx does not bind DNA directly, HBx activates Ras/mitogen-activated protein kinase pathways including extracellular signal-regulated kinase and c-Jun N-terminal kinase (JNK),[7] resulting in tumor cell growth and survival.

Transforming growth factor β (TGF-β) can inhibit epithelial cell growth, acting as a tumor suppressor. During carcinogenesis, however, cancer cells gain advantage by selective reduction of the tumor-suppressive activity of TGF-β together with augmentation of its oncogenic activity.[8] This led us to hypothesize that alterations in the TGF-β signal transduction pathway could be involved in the development of HCC in long-standing HBV infection.

Smads are central mediators of signals from the receptors for TGF-β superfamily members to the nucleus.[9] Smads are modular proteins with conserved Mad-homology 1, intermediate linker, and Mad-homology 2 domains.[10] The catalytically active TGF-β type I receptor (TβRI) phosphorylates the C-terminal serine residues of receptor-activated Smads, which include Smad2 and the highly related protein Smad3. The linker domain can undergo regulatory phosphorylation by other kinases including mitogen-activated protein kinases and cyclin-dependent kinases.[11-14] In contrast to the clearly activating role of the C-terminal phosphorylation events, the regulation of Smad activity by phosphorylation of the linker region is complex. Linker phosphorylation of Smad2 during human colorectal carcinogenesis results in cytoplasmic retention of Smad2 and inhibition of tumor-suppressive TGF-β signaling.[11,15] However, Smad3 phosphorylated at the linker region (pSmad3L) is localized predominantly to cell nuclei in actively growing Ki-67–immunoreactive colon cancer with distant metastasis.[15] Reversible shifting of Smad-dependent signaling between tumor suppression and oncogenesis in hyperactive Ras-expressing cells indicates that Smad3 phosphorylated at the C-terminal region (pSmad3C) transmits a tumor-suppressive TGF-β signal, whereas oncogenic activities such as cell proliferation and invasion are promoted by the pSmad3L pathway.[16] In addition, Roberts' group[17] has recently reported that Smad3 is critical for Ras/JNK-mediated transformation. Taken together, these findings indicate that oncogenic TGF-β signaling results from the functional collaboration of Ras and Smad3 rather than from Ras-mediated inhibition of the Smad3 pathway. Linker phosphorylation of Smad3 indirectly inhibits C-terminal phosphorylation, minimizing tumor-suppressive pSmad3C signaling.[16] Notably, pSmad3L-mediated signaling in activated hepatic stellate cells (HSCs) promotes liver fibrosis by stimulating extracellular matrix deposition.[13,18]

The role of HBV and HCV in tumor formation appears to be complex and may involve both direct and indirect mechanisms.[19] Integration of HBV DNA into the host genome occurs at early steps of clonal tumor expansion. Alternatively, chronic liver inflammation and hepatic regeneration induced by host cellular immune responses can increase the risk of HCC development. During progression of HCV-related chronic liver disorders, hepatocytes affected by chronic inflammation undergo a transition from the tumor-suppressive pSmad3C pathway to the JNK/pSmad3L pathway.[20] Our present studies extend the previous observations to HBV-related hepatocarcinogenesis. We study Smad3 phosphorylation profiles in HBV-infected human liver and HBx transgenic mouse liver, concluding that HBx oncoprotein in early stages of chronic hepatitis B contributes directly to hepatocarcinogenesis by shifting hepatocytic Smad3-mediated signaling from tumor suppression to oncogenesis.

Patients and Methods

Patients, Follow-up, and Detection of HCC. Ninety patients with HBV-related chronic liver disease underwent liver biopsy at the Department of Gastroenterology and Hepatology of Kansai Medical University Hospital between 1992 and 1994. All patients were seropositive for hepatitis B surface antigen (Abbott Laboratories, North Chicago, IL) and were seronegative for anti-HCV antibody (Ortho Diagnostics, Tokyo, Japan). Patients included 70 with chronic hepatitis, 10 with cir-

Address reprint requests to: Koichi Matsuzaki, M.D., Departments of Gastroenterology and Hepatology, Kansai Medical University, 10-15 Fumizonocho, Moriguchi, Osaka, 570-8507, Japan. E-mail: matsuzak@takii.kmu.ac.jp; fax: (81)-6-6996-4874.

Copyright © 2008 by the American Association for the Study of Liver Diseases.

Published online in Wiley InterScience (www.interscience.wiley.com).

DOI 10.1002/hep.22765

Potential conflict of interest: Nothing to report.

Additional Supporting Information may be found on the online version of this article.

rhosis, and 10 with HCC. Sixty of the chronic hepatitis patients were enrolled in a program for early diagnosis of HCC; the other 10 were lost to follow-up. HBV DNA (Roche Diagnostics, Tokyo, Japan) and hepatitis B envelope antigen (Abbott Laboratories) were measured at the time of liver biopsy. During the surveillance period, patients were followed up with abdominal ultrasonography and plasma alpha-fetoprotein determinations every 3 to 6 months. We also made a random choice of 20 chronic hepatitis B specimens with little fibrosis (F1) and little inflammation (A1) from the liver biopsy specimens of the patients showing high plasma HBV DNA levels.

Necroinflammatory activity and fibrotic stage were graded histologically according to the classification of Desmet and colleagues.[21] We counted and scored pSmad3, HBx, and c-Myc positivity in hepatocytes as follows: 0, no positivity; 1, <25%; 2, 25% to 50%; 3, 50% to 75%; 4, >75%.[20] Written informed consent was obtained from each patient according to the Helsinki Declaration. We also obtained approval for this study from our institutional ethics committee.

Reverse-Transcription Polymerase Chain Reaction. Reverse-transcription polymerase chain reaction of TGF-β type II receptor (TβRII), Smad2, and Smad4 genes was performed as described.[15]

Domain-Specific Antibodies Against the Phosphorylated Smad3. Two polyclonal anti-phospho–Smad3 sera—α pSmad3L (Ser 208/213) and α pSmad3C (Ser 423/425)—were raised against the phosphorylated linker and C-terminal regions of Smad3 by immunization of rabbits with synthetic peptides. Relevant antisera were affinity-purified using phosphorylated peptides as described.[13]

Transgenic Animals. HBx transgenic mice were derived by microinjection of a 1151-bp HBV DNA fragment containing the HBx gene with its own regulatory elements and polyadenylation signal into fertilized eggs of CD-1 mice. An independent line (H9) was derived from founders.[6]

Immunohistochemical and Immunofluorescence Analyses. Immunohistochemical and immunofluorescence analyses were performed as described.[18] Primary antibodies (Abs) used in this study included mouse monoclonal anti-HBx Ab (2 μg/mL; Abcam, Cambridge, UK), mouse monoclonal anti-c-Myc Ab (10 μg/mL; Santa Cruz Biotechnology, Santa Cruz, CA), and mouse monoclonal anti-$p21^{WAF1}$ Ab (0.5 μg/mL; DAKO, Glostrup, Denmark), in addition to the affinity-purified rabbit polyclonal anti-pSmad3L (2 μg/mL) and anti-pSmad3C (0.5 μg/mL) as described above. Anti-pSmad3C Ab cross-reacted weakly with C-terminally phosphorylated Smad2: to block binding of anti-pSmad3C Ab to phosphorylated domains in Smad2, anti-pSmad3C Ab was adsorbed with 1 μg/mL C-terminally phosphorylated Smad2 peptide.

For immunohistochemical analyses, sections exposed to primary Abs were then incubated with peroxidase-labeled polymer conjugated to goat anti-mouse or anti-rabbit immunoglobulin G (IgG) (DAKO). Finally, sections were developed with 3,3'-diaminobenzidine tetrahydrochloride (DAB; Vector Laboratories, Burlingame, CA), counterstained with Mayer's hematoxylin (Merck, Darmstadt, Germany), and mounted under coverslips.

For double-labeling immunofluorescence analyses, sections exposed to a pair of primary Abs (rabbit plus mouse) were then incubated in a 1:500 dilution of goat anti-rabbit IgG conjugated with a red fluorophore (Alexa Fluor 594; Molecular Probes, Eugene, OR) and goat anti-mouse IgG conjugated with a green fluorophore (Alexa Fluor 488; Molecular Probes). Images were obtained with a fluorescence microscope (Carl Zeiss Microimaging, Oberkochen, Germany).

Immunoprecipitation and Immunoblotting. pSmad3L and pSmad3C immunoblots on Smad3 immunoprecipitates of cell extracts from frozen tissues representing either HCC or underlying liver diseases were performed as described.[20]

In Vitro *Kinase Assay.* *In vitro* kinase assay was performed as described.[12]

Statistical Analyses. The Kaplan-Meier method was used to determine the cumulative probability of appearance of HCC during the 12-year follow-up period. HCC occurrence curves were compared between patients with abundant (scores 3 to 4) and those with sparse (scores 0 to 2) Smad3L/C phosphorylation, by means of the log-rank test. For continuous variables, the optimal cutoff threshold for defining groups was established using receiver operating characteristics curves. All parameters with *P* values less than 0.10 in the univariate analysis were selected for multivariate analysis, which was performed using the Cox proportional hazards model.[22] *P* values less than 0.05 were considered significant. The Mann-Whitney U test was used to identify significant differences in hepatocytic pSmad3L and pSmad3C positivity among fibrotic stages.

Results

Two Distinct Hepatocytic Smad3 Signaling Pathways in Human Chronic Hepatitis B: pSmad3L- and pSmad3C-Dominant Types. We initially analyzed mutations of TβRII, Smad2, and Smad4 genes in 10 HCC and six cirrhotic liver samples, finding no mutations in

Table 1. Clinicopathologic Features, Smad3L/C Phosphorylation, and HBx and c-Myc Positivities in Specimens from Patients with HBV-Related Chronic Liver Disease

		Fibrotic Stage*				
	Nomal	F1	F2	F3	F4	HCC
Patients, n	2	20	27	23	10	10
Sex (male/female), n	2/0	13/7	19/8	17/6	5/5	10/0
Age (years), mean ± SD	57.0 ± 9.9	35.5 ± 14.3	34.3 ± 13.9	43.1 ± 13.7	59.6 ± 7.6	54.0 ± 15.1
pSmad3L staining, n†						
0	2	0	0	0	0	0
1	0	8	6	2	1	0
2	0	6	6	7	1	0
3	0	3	11	11	2	5
4	0	3	4	3	6	5
pSmad3C staining, n†						
0	0	0	0	0	0	0
1	0	0	4	4	2	4
2	0	4	9	12	7	3
3	2	11	7	5	1	3
4	0	5	7	2	0	0
Activity, n*						
A0	2	1	0	0	0	0
A1	0	17	6	1	0	1
A2	0	2	19	11	3	7
A3	0	0	2	11	7	2
HBx staining, n†						
0	2	0	0	0	1	1
1	0	6	5	3	2	3
2	0	7	11	8	3	3
3	0	3	7	6	2	2
4	0	4	4	6	2	1
c-Myc staining, n†						
0	2	0	0	0	0	0
1	0	2	4	1	1	0
2	0	9	10	8	3	1
3	0	6	8	8	3	3
4	0	3	5	6	3	6
Histology of HCC (well/moderate)‡						6/4
TNM stage (I/II/III/IV)ʃ						4/4/2/0
Size of tumor (cm), mean ± SD						2.2 ± 0.3
AST (IU/L), mean ± SD	22.5 ± 3.5	68.6 ± 56.1	92.8 ± 65.8	79.7 ± 51.8	82.0 ± 53.1	71.0 ± 36.4
ALT (IU/L), mean ± SD	24.0 ± 2.8	104 ± 83.5	141 ± 97.5	84.5 ± 83.1	68.2 ± 52.3	59.1 ± 32.2
Platelet count (× 10^9/L), mean ± SD	25.0 ± 4.2	17.1 ± 3.6	15.8 ± 4.9	14.1 ± 7.1	9.7 ± 6.7	9.0 ± 3.7
AFP (ng/mL), mean ± SD	2.1 ± 1.3	6.8 ± 4.6	14.8 ± 12.2	66.2 ± 138	132 ± 208	164 ± 184

Abbreviations: AFP, alpha-fetoprotein; ALT, alanine aminotransferase; AST, aspartate aminotransferase; pSmad3L, linker-phosphorylated Smad3; pSmad3C, C-terminally phosphorylated Smad3; SD, standard deviation; TNM, tumor-node-metastasis.

*Necroinflammatory activity and fibrotic stage are determined histologically according to Desmet's classification.

†Hepatocytic Smad3 phosphorylation is scored as follows: 0, no phosphorylation; 1, <25% Smad3 phosphorylation; 2, 25% to 50% Smad3 phosphorylation; 3, 50% to 75% Smad3 phosphorylation; 4, >75% Smad3 phosphorylation. Extent of HBx and c-Myc expression is indicated as that of pSmad3L positivity.

‡Histological grading of HCC is classified according to the criteria of the International Working Party.

ʃTNM is classified by the International Union Against Cancer and American joint Committee on Cancer.

any sample. This confirms the low probability of mutations in HCC tissues, which has been reported recently.[23]

To investigate domain-specific phosphorylation mediating Smad3 signaling *in vivo*, we generated two Abs specific to each phosphorylation site, and determined the distribution of pSmad3L and pSmad3C in chronic hepatitis B and C specimens. Table 1 shows clinical background and positivity for pSmad3L and pSmad3C in 90 patients with HBV-related chronic liver diseases. We also studied HCC occurrence over 12 years in 60 patients with chronic hepatitis B who were enrolled in a program for early diagnosis of HCC (Table 2). We recently reported that Smad3 was phosphorylated at the linker region, particularly in groups of hepatocytes adjoining collagen fibers in portal tracts in chronic hepatitis C.[20] In contrast, the distribution of pSmad3L and pSmad3C in chronic

Table 2. Clinicopathologic Features, Smad3L/C Phosphorylation, and HCC Incidence in Specimens from Patients with HBV-Related Chronic Hepatitis

Patient No.	Sex	Age	Incidence of HCC	pSmad3L Staining*	pSmad3C Staining*	Fibrotic Stage†	Inflammatory Activity†	HBV DNA (log copies/mL)	HBeAg
1	M	62	○	4	2	3	3	5.4	+
2	F	44	○	4	2	2	2	5.5	−
3	M	22	○	4	2	2	2	5.2	−
4	F	20		4	4	3	3	3.0	−
5	M	43		4	4	2	2	4.5	−
6	M	30		4	2	2	3	4.0	−
7	M	30		4	2	2	3	5.6	−
8	M	65	○	3	2	3	3	4.0	+
9	F	56	○	3	2	3	2	3.7	+
10	M	52	○	3	1	1	1	6.4	−
11	F	40		3	1	1	1	6.9	−
12	M	44		3	1	3	3	5.1	−
13	M	45		3	1	3	3	3.8	−
14	M	28		3	2	3	1	3.0	−
15	M	60		3	2	3	2	2.8	−
16	M	44		3	2	3	3	5.2	+
17	M	44		3	2	3	3	3.2	+
18	M	44		3	2	3	3	4.4	−
19	F	26		3	2	2	1	4.9	−
20	M	20		3	2	2	1	2.9	+
21	M	59		3	2	2	2	4.4	−
22	M	43		3	3	2	2	3.2	+
23	M	29		3	3	3	2	6.2	−
24	M	29		3	3	3	2	3.0	−
25	M	25		3	4	1	1	3.5	−
26	F	33		3	4	2	2	4.6	+
27	M	19		3	3	3	2	5.6	−
28	M	63		3	4	2	2	5.1	−
29	M	52	○	2	1	3	2	3.7	−
30	M	44		2	2	3	3	5.2	−
31	M	29		2	2	3	2	3.9	+
32	F	46		2	4	3	3	3.2	−
33	M	25		2	2	1	2	5.0	−
34	F	23		2	3	1	1	2.1	−
35	F	31		2	3	2	2	3.9	+
36	F	26		2	3	1	1	2.4	−
37	M	35		2	3	1	1	5.6	−
38	M	20		2	3	2	1	3.2	+
39	F	56		2	3	3	2	5.1	+
40	F	36		2	3	3	2	2.6	−
41	F	25		2	3	2	1	5.1	−
42	F	23		2	4	2	1	3.5	−
43	F	41		2	4	1	1	2.0	+
44	M	29		2	4	2	2	4.5	−
45	M	31		2	4	1	1	5.9	+
46	M	42		2	1	2	2	3.7	−
47	M	24		1	1	2	2	3.9	+
48	M	28		1	2	3	2	3.8	−
49	F	11		1	2	2	2	3.0	+
50	M	40		1	1	2	2	3.2	−
51	M	37		1	2	2	2	3.0	−
52	F	10		1	2	2	2	2.3	−
53	M	16		1	3	1	1	5.1	−
54	M	41		1	3	1	1	4.3	−
55	M	40		1	3	1	1	2.2	−
56	M	53		1	3	1	1	2.7	−
57	M	27		1	3	1	1	4.6	−
58	M	53		1	4	1	1	3.3	−
59	M	30		1	4	2	2	2.1	−
60	F	22		1	4	1	0	3.7	−

Abbreviations: F, female; HBeAg, hepatitis B e antigen; HBV, hepatitis B virus; HCC, hepatocellular carcinoma; M, male; pSmad3C, C-terminally phosphorylated Smad3; pSmad3L, linker-phosphorylated Smad3.

*Hepatocytic Smad3 phosphorylation is scored as follows: 0, no phosphorylation; 1, <25% Smad3 phosphorylation; 2, 25% to 50% Smad3 phosphorylation; 3, 50% to 75% Smad3 phosphorylation; 4, >75% Smad3 phosphorylation.

†Necroinflammatory activity and fibrotic stage are determined histologically according to Desmet's classification.

hepatitis B specimens was divided into two distinct patterns. In one liver specimen with moderate fibrosis and inflammation from patient 2 in Table 2 who was diagnosed with HCC 9 years later, intense pSmad3L immunostaining was present in the nuclei of all hepatocytes throughout the liver lobules; C-terminal phosphorylation of Smad3 was strongly suppressed in hepatocytic nuclei (Fig. 1A and Supplementary Fig. 1). In another specimen with similar fibrotic stage and necroinflammatory activity from patient 44 in Table 2 who had not developed HCC, many hepatocytes retained phosphorylation at Smad3C but showed scarce phosphorylation at Smad3L (Fig. 1B). Among 37 patients with chronic hepatitis B who had strong pSmad3L positivity, 24 patients showed little Smad3C phosphorylation, and only 13 patients showed abundant Smad3C phosphorylation (64.9% versus 35.1% [$P = 0.03$]) (Table 3). In contrast, 22 patients with little Smad3L phosphorylation (scores 0 to 2) versus only 13 patients with abundant Smad3L phosphorylation (scores 3 to 4) showed strong pSmad3C positivity (62.9% versus 37.1% [$P = 0.04$]). Because the extent of Smad3L phosphorylation increased as fibrotic stage and necroinflammatory activity progressed in chronic hepatitis C, Smad3L showed little phosphorylation in early chronic hepatitis C.[20] In contrast, degree of linker phosphorylation of Smad3 in hepatocytic nuclei remained high (staining scored as 3 or 4) in 21 of 47 patients with chronic hepatitis B (F1 to F2) (Fig. 1C). These results indicate differential mechanisms of HBV- and HCV-

Table 3. Correlation Between pSmad3L and pSmad3C in Chronic Hepatitis B Specimens

	pSmad3C Positivity *		
	Low (1 and 2)	High (3 and 4)	Total
pSmad3L positivity *			
Low (1 and 2)	11	22	33
High (3 and 4)	24	13	37
Total	35	35	70

Abbreviations: pSmad3C, C-terminally phosphorylated Smad3; pSmad3L, linker-phosphorylated Smad3.

*Hepatocytic Smad3 phosphorylation is scored as follows: 0, no phosphorylation; 1, <25% Smad3 phosphorylation; 2, 25% to 50% Smad3 phosphorylation; 3, 50% to 75% Smad3 phosphorylation; 4, >75% Smad3 phosphorylation.

COLOR

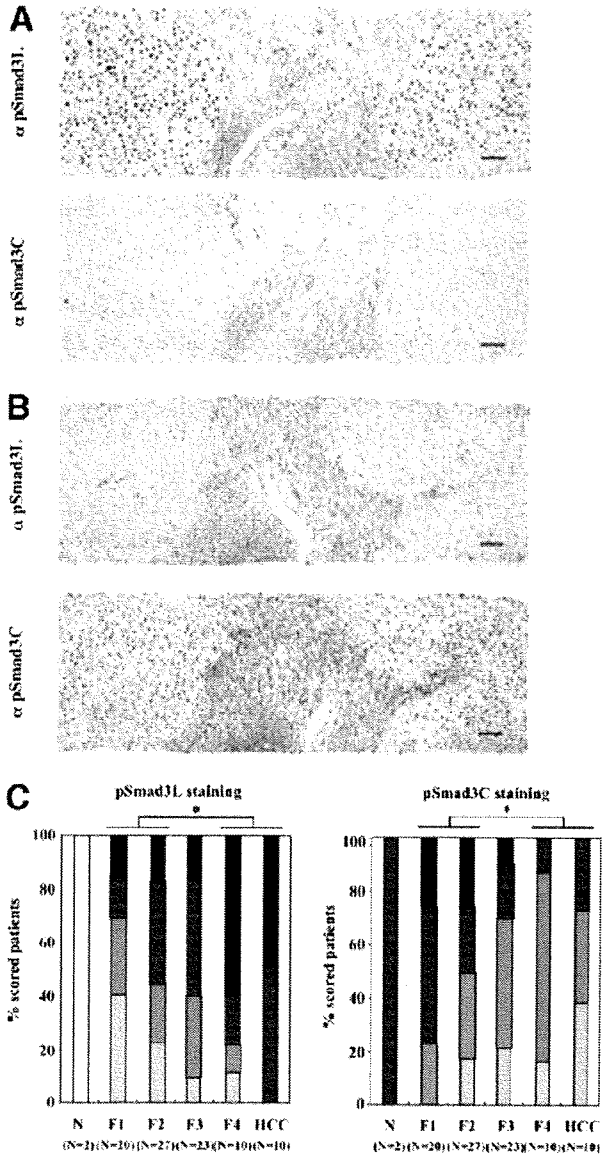

Fig. 1. Two distinct hepatocytic Smad3 signaling pathways in early chronic hepatitis B: pSmad3L- and pSmad3C-dominant types. (A) Smad3 in the nuclei of hepatocytes was phosphorylated sparsely at the C-terminal region (α pSmad3C column) but intensely at the linker region (α pSmad3L column). The liver specimen showing moderate fibrosis and inflammation was obtained from patient 2 in Table 2 diagnosed with HCC 9 years later. Bar = 50 μm. (B) In patient 44 in Table 2 who had not developed HCC, hepatocytes retained phosphorylation at Smad3C (α pSmad3C column) but showed little phosphorylation at Smad3L (α pSmad3L column). The specimen showed degrees of fibrosis and necroinflammatory activity similar to those in (A). Formalin-fixed, paraffin-embedded liver sections were stained with anti-pSmad3L Ab (α pSmad3L column) and anti-pSmad3C Ab (α pSmad3C column). The pSmad3C section was paired with an adjacent section stained using anti-pSmad3L Ab. Abs were then bound by goat anti-rabbit IgG conjugated with peroxidase-labeled polymer. Peroxidase activity was detected with 3,3'-diaminobenzidine tetrahydrochloride. All sections were counterstained with hemotoxylin (blue). Brown color indicates specific Ab reactivity. Bar = 50 μm. (C) Degrees of Smad3 phosphorylation were stable in hepatocytic nuclei in early chronic hepatitis B specimens (F1 to F2), whereas pSmad3L increased and pSmad3C decreased as chronic hepatitis B (F3) progressed through cirrhosis to HCC. Smad3 phosphorylation in hepatocytes did not change between F1 and F2 stages. Phosphorylation of Smad3L and Smad3C in hepatocytes of cirrhotic liver (F4) and HCC was greater and less than that in livers with grade F1 and F2 fibrosis, respectively. Extent of Smad3 phosphorylation: □, 0; ⊔, 1; ▨, 2; ▩, 3; ■, 4. *$P < 0.05$.